LINEARIZATION AND HEALTH ESTIMATION OF A TURBOFAN ENGINE

BHARATH REDDY ENDURTHI

Bachelor of Engineering in Electronics and Instrumentation Engineering

University of Madras, India

June, 2001

Submitted in partial fulfillment of requirements for the degree

MASTER OF SCIENCE IN ELECTRICAL ENGINEERING

at the

CLEVELAND STATE UNIVERSITY

December, 2004

LINEARIZATION AND HEALTH ESTIMATION OF A TURBOFAN ENGINE

BHARATH REDDY ENDURTHI

ABSTRACT

Jet engines are precision machines composed of many expensive parts characterized by a large number of variables. An engine's health deteriorates considerably over time. Certain engine variables, known as health parameters, have a major effect on its health. Monitoring and evaluating these health parameters help in developing predictive control techniques and maintenance, thereby increasing the performance, life, reliability, and safety of the engine. The main aim of this research is to estimate the health parameter deterioration of a turbofan aircraft engine over a period of time. It is impossible to directly measure the health parameters. We therefore estimate the health parameters using an estimation technique based on the available measurements. The Kalman filter has been shown to be an optimal estimator for linear systems. So the nonlinear engine model is linearized with respect to three different sets of parameters (states, controls, and health parameters) using three different linearization methods. This gives us 27 different possible linear models for one nonlinear engine model. The different linearization methods that will be discussed are the Matlab method, the perturbation method, and the steady state error reduction method. Kalman filtering results are investigated for all 27 different linear models at two different operating conditions for the turbofan engine. A graphical user interface is also developed to make the turbofan health estimation problem more user friendly. The implementation of the unscented Kalman filter, a new nonlinear estimation technique, is also discussed.

ACKNOWLEDGEMENT

I would like to express my sincere indebtness and gratitude to my thesis advisor Dr. Dan Simon, for the ingenious commitment, encouragement and highly valuable advice he provided me over the entire course of this thesis. I would like to thank Sanjay Garg and Donald Simon at the NASA Glenn Research Center, and the NASA Aviation Safety Program, for generously providing funding for this work.

I would also like to thank my committee members Dr. Zhiqiang Gao and Dr. Sridhar Ungarala for their support and advice.

I wish to thank my lab mates at the Embedded Control Systems Research Laboratory for their encouragement and intellectual input during the entire course of this thesis without which this work wouldn't have been possible.

Finally, I wish to thank my roommates and all my friends who have always been a constant source of inspiration to me.

To my parents Smt. & Sri. E. Vijaya Reddy

TABLE OF CONTENTS

PAGE

LIST OF FIGURES……ix

LIST OF TABLES……..xi

CHAPTER I – INTRODUCTION……..1

CHAPTER II – THE TURBOFAN ENGINE……..4

2.1 Jet propulsion theory……...5

2.2 Gas turbine engine (Turbojet)……..…7

2.2.1 Components of the jet engine……..8

2.2.2 Types of jet engines……10

2.2.3 Jet engines with afterburners……13

2.3 Engine performance……...14

2.3.1 Engine rating……..14

2.3.2 Engine maintenance……...15

2.3.3 Engine performance deterioration……15

2.4 Turbofan engine used in this research (MAPSS)……..16

2.5 Engine's state space model……....22

CHAPTER III – LINEAR STATE ESTIMATION……25

3.1 Different estimation techniques……..26

3.1.1 Least squares estimation…….26

3.1.2 Weighted least squares estimation……...28

3.1.3 Bayesian estimation……..29

3.1.4 Recursive least squares estimation……...30

3.2 State estimation in a linear system……...35

3.3 Discrete time Kalman filter……..37

CHAPTER IV – LINEARIZED KALMAN FILTER……...43

4.1 Nonlinear estimation…….44

4.1.1 Linearized Kalman filter……....44

4.1.2 Extended Kalman filter……..47

4.2 Linearization…….49

4.2.1 Matlab linearization……...50

4.2.2 Perturbation linearization…….….51

4.2.2a Linearization with respect to states……..51

4.2.2b Linearization with respect to control inputs.....52

4.2.3 Steady state error reduction method……...53

4.2.3a Linearization with respect to states…….…..53

4.2.3b Linearization with respect to controls……...54

4.3 Linearization of the MAPSS turbofan engine model…….....55

4.4 Discretization of the MAPSS linear model……....56

4.5 Discrete Linearized Kalman filter…….….58

4.6 Health estimation graphical user interface…….....60

CHAPTER V – SIMULATION RESULTS……62

5. 1 Linearization of the MAPSS turbofan engine model……...63

5. 2 Health parameter estimation results…….70

5.2.1 Unconstrained Kalman filter estimates…….72

5.2.2 Constrained Kalman filter estimates…….75

CHAPTER VI – UNSCENTED KALMAN FILTER……82

6.1 Unscented transformation……..84

6.2 Unscented Kalman filter……87

6.2.1 Algorithm for additive noise……...89

6.2.2 Algorithm for non-additive noise……92

6.3 Sigma point selection analysis……...93

6.3.1 Algorithm for minimal skew simplex sigma point set…….95

6.3.2 Algorithm for spherical simplex sigma point set……97

6.4 Inverted pendulum application……..98

6.5 Simulation results…….101

CHAPTER VII – CONCLUSIONS AND FUTURE WORK……...104

7.1 Conclusions……...104

7.2 Future work……...106

BIBLIOGRAPHY……108

LIST OF FIGURES

FIGURE ……PAGE

2.1 Inflated balloon……5

2.2 Inflated balloon with stem released…….....5

2.3 Heron's aeolipile……..…6

2.4 Turbojet…….....10

2.5 Turboprop/ Turboshaft……..11

2.6 Turbofan…….....12

2.7 Schematic of turbofan engine model…….....17

2.8 MAPSS block diagram (Module Interaction)…….…...18

2.9 Component level model with engine components…….....20

2.10 MAPSS graphical user interface…….…….21

3.1 Mean and covariance propagation…….……40

4.1 Health estimation graphical user interface…….....61

5.1 RMS errors of 27 linear models…….....66

5.2 Linear vs Nonlinear simulations……....68

5.3a Unconstrained RMS health parameters degradation estimation errors for 1st operating condition……...74

5.3b Constrained RMS health parameters degradation estimation errors for 1st operating condition……...76

5.4a Unconstrained health parameter degradation estimates…….…...79

5.4b Constrained health parameter degradation estimates…….…...80

5.5a Unconstrained RMS health parameters degradation estimation errors for 2nd operating condition……..81

5.5b Constrained RMS health parameters degradation estimation errors for 2nd operating condition …….81

6.1 Principle of Unscented transformation……..…87

6.2 Mean and covariance propagation in three different transformations……...88

6.3 Inverted pendulum…….....98

6.4a Estimation of position and velocity of the cart…….....102

6.4b Estimation of angle and angular velocity of the pendulum……103

LIST OF TABLES

TABLE…… ……..PAGE

I – Best RMS errors averaged over the entire simulation time…….65

II – Best RMS errors at the final time…….....66

III – Linear models performance…….....69

IV – RMS health parameter estimation errors for the unconstrained Kalman filter

for *27* linear models…..……..73

V – RMS health parameter estimation errors for the constrained Kalman Filter

for *27* linear models…….....77

CHAPTER I

INTRODUCTION

Jet engine components are subject to degradation over their lifetime of use [1]. This degradation affects the fuel economy and component life consumption of the turbine. Performance data is collected periodically to evaluate (estimate) the health of the engine. This evaluation (estimation) is then used to decide maintenance schedules. This offers the benefits of improved safety and reduced operating costs. The data used for the health evaluation is collected during the flight and analyzed post flight for maintenance schedules. Various algorithms have been proposed to estimate the health parameters of a jet engine such as weighted least squares [2], expert systems [3], neural networks [4], Kalman filters [4] and genetic algorithms [5]. The research work presented here deals with the application of Kalman filters for health parameter estimation.

The main aim of this thesis is to investigate various linearization techniques that can be implemented to linearize the highly nonlinear turbofan engine model and then to estimate its health parameters. Different estimation techniques like linearized Kalman

filter and unscented Kalman filter are to be implemented to estimate the engine health parameters. Once the linear models are validated, their effects on the engine health parameter estimates are checked. A graphical user interface for the implementation for health parameter estimation of turbofan engine has to be developed. The implementation of unscented Kalman filter, a new nonlinear estimation technique, for the turbofan engine health parameter estimation is also discussed.

A turbofan engine model can be obtained from the basic knowledge of physics of a turbofan. Chapter II discusses the working principle of a turbofan engine and also describes the different kinds of turbofan engines. MAPSS (modular aero propulsion system simulation) is the engine model used in this research. MAPSS is a prototype (dynamic model) of a high pressure ratio, dual spool, low bypass military type turbofan engine [6].

State estimation plays an important role in the field of control engineering. Dynamic measurements from the system are considered while estimating the states of the corresponding system. The basic estimation techniques implemented for the linear systems are described in Chapter III. The Kalman filter has been applied in areas as diverse as aerospace, marine navigation, nuclear power plant instrumentation, demographic modeling, manufacturing, and many others. This filter, also considered to be the optimal state estimator, is also discussed.

As the turbofan engine is highly nonlinear, linear estimation cannot be directly implemented. Hence, nonlinear estimation techniques which are derived from the linear state estimation are also discussed. The linearized Kalman filter, considered to be one of the efficient nonlinear estimation techniques, is derived in Chapter IV. This nonlinear estimation technique works on the linearized model of the nonlinear model. Hence the linearization process and different kinds of linearization techniques are also discussed in Chapter IV.

The implementation of the linearized Kalman filter to the turbofan engine is discussed is Chapter VI. Various linear models of the MAPSS model are obtained and their behavior is compared with the nonlinear MAPSS model. The results of the implementation of the linearized Kalman filter with all of the linear models are shown.

Lots of research is being carried out in nonlinear estimation. The unscented Kalman filter, a new estimation technique, is one result of that research [7]. The unscented Kalman filter is derived to overcome the difficulties faced in the implementation of the extended or linearized Kalman filter. Chapter VI discusses the unscented Kalman filter and its application to a small state problem. The implementation of the unscented Kalman filter for the turbofan model is discussed in Chapter VII.

CHAPTER II

THE TURBOFAN ENGINE

One should be able to understand the basic theories and terms of turbofan engines while working with them. The turbofan engine works on jet propulsion theory. Propulsion is the net force that results from unbalanced forces. These unbalanced forces are the result of implementation of Newton's laws of motion to certain objects. Gas (air) under pressure in a sealed container exerts equal pressure on all surfaces of the container, therefore, all the forces are balanced and there are no forces to make the container move. If there is a hole in the container, gas (air) cannot push against that hole and thus the gas escapes. While the air is escaping, the side of the container opposite to the hole has more pressure than side with the hole. Therefore, the net pressures are not balanced and there is a net force available to move the container. This principle is better explained with an inflated balloon (container). A brief introduction of the jet propulsion theory is given in Section 2.1. The working principle of gas turbine engine and different types of gas turbine engines are discussed in Section 2.2. Section 2.3 explains the engine performance, and is immediately followed by Section 2.4 which describes the turbofan engine used in this research. Finally Section 2.5 describes the modeling of the turbofan engine.

2.1 Jet propulsion theory

Consider a balloon on a table, inflated with air at room temperature and the stem is held closed so that no air can escape. The balloon remains motionless as shown in Figure 2.1 since the air pressure inside the balloon is pressing equally on the balloon skin in all directions. That is, there is no force exerted on the balloon to move it.

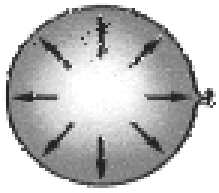

Figure 2.1: Inflated balloon

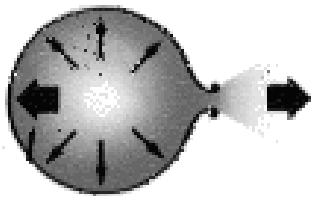

Figure 2.2: Inflated balloon with stem released

However, when the stem of the balloon is released, the air escapes through the opening created by the stem release as shown in Figure 2.2. This process also creates an unbalance in the pressures acting on the skin of the balloon. The pressure at the stem section of the balloon reduces, but the pressure on opposite section to the skin doesn't change. This pressure imbalance results in unbalanced forces acting on the balloon, which makes the balloon move forward in direction opposite to the stem opening through which the air escapes. The force with which the balloon moves forward is called *thrust*. All the reaction engines like gas turbine engine, rocket, pulsejet or ramjet work on the same principle described above. However, the important thing to be noted is that the balloon would have moved even if the room had been a large vacuum chamber. That is, the thrust developed does not need any medium to move the balloon. Rockets in general operate on the same principle as they travel in the airless outer space. The major principle

being the conversion of the energy of expanding air (gases) in to mechanical force (thrust).

Heron of Alexandria (Hero) built the first reaction engine somewhere around 250 B.C. Heron devised a machine called aeolipile shown in Figure 2.3, which was a closed vessel in the shape of a sphere with two bent tubes mounted on its surface opposite to each other. Steam at very high pressure was continuously introduced in to the sphere. The high pressure steam escaped through the two tubes resulting in a force rotating the sphere about an axis. The principle behind this phenomenon was not fully understood until 1690 A.D. when Sir Isaac Newton in England formulated the principle of Hero's jet propulsion "aeolipile" in scientific terms. His Third Law of Motion stated: "Every action produces a reaction ... equal in force and opposite in direction."

Figure 2.3: Heron’s aeolipile

All the jet engines designed operate on the same principle. Although there are piston engines which work similar to the jet engines, they are rarely used in the aircrafts. Both the engines convert the energy of the expanding gases in to mechanical force (thrust). The major drawback in the piston engines is that they impart relatively small

acceleration to a large mass of air compared to the large acceleration of small mass of air in jet engine case.

2.2 Gas turbine engine (Turbojet)

The gas turbine engine is the turbine engine that is operated by a gas, which is the product of the combustion that takes place when a fuel is mixed and burned with the air passing through the engine. Jet engine is the other name for gas turbine engine. The operation of the turbojet; simplest gas turbine engine is similar to that of the aeolipile. However, the sphere is replaced by a can like horizontal container open at both ends. This horizontal container is called an engine case. This engine case has five major sections like inlet, compressor, combustor (burner), turbine and outlet (jet nozzle). Large quantities of air enter the engine through the inlet. The air entered then passes through the compressor to attain high pressures. The temperature of the high pressure air is increased by burning (mixing) it with the fuel in the combustor. The combustion results in high velocity hot gases which pass through the turbines, generating power to run the compressor. These high velocity hot gases coming out of the turbine are exhausted to the outside through the outlet (jet nozzle) creating a thrust to the move the horizontal container (engine) forward. It is out of the scope of this research to discuss details of all of the chemical, thermo dynamical or mechanical reactions involved in an engine model.

2.2.1 Components of the jet engine

The working principle of a turbofan described above would be more clearly understood by studying its main parts. There are five main parts of a turbofan or any gas turbine engine, which play an important role in the engine's operation.

a) Inlet

Air enters in to the engine through the inlet. The main task of the inlet is to straighten out the flow, making it uniform and without much turbulence. This is important because compressors and fans need to be fed distortion-free air. Inlet is positioned just before the compressor. There are different types of inlets based on the speed of the aircraft like subsonic inlets, supersonic inlets and hypersonic inlets.

b) Compressor

A compressor is used to increase the pressure of the air entering through the inlet. The air is forced through several rows of both spinning and stationary blades. As the air passes each row, the available space is greatly reduced, and so the air that exits this phase is thirty or forty times higher in pressure than it was outside the engine. The temperature of the air also gets increased because of the increase in pressure. Axial flow compressor and centrifugal compressor are the two main types of computers used in turbofan engines. The compressor is mounted in front of the combustor.

c) Burner (combustor)

The burner is the component in which the actual reaction (combustion) takes place. The high pressure hot air coming out of the compressor is combined with the fuel and burned for combustion. The combustion results in very high temperature gases with high velocities. These high temperature exhaust gases are used to drive the turbine.

Burners, placed just after the compressors, are made from materials that can withstand the high temperatures of combustion. Annular, can, can-annular burners are the three different types of burners mostly used.

d) Turbine

The turbine is located next to the burner. The power used to drive the compressors is obtained from turbines. The turbine extracts the energy of the high temperature gas flow coming out of the burner by rotating the blades. This energy is transferred to the compressors by connecting shafts. The air leaving the turbine has low temperature and pressure when compared with the air coming out of the burner because of the energy extraction. Turbine blades must be made of special materials that can withstand the heat, or they must be actively cooled. There can be multiple turbine stages for driving different parts of the engine independently like compressor, fan (turbofan) or propeller (turboprop).

e) Nozzle (exhaust)

A nozzle is a specially shaped tube through which the hot gases flow. The actual thrust required to move the engine forward is produced in this nozzle which is positioned after the turbine stage in the engine. The thrust is developed by conducting the hot exhaust gases through this nozzle to the free stream of outside air. Like the air leaving a balloon described in the Section 2.1, the speed and flow rate of the air leaving the nozzle provides the airplane with thrust. Both the temperature and pressure of the air or rather hot gases is reduced very much while passing through the nozzle. The inside walls of the nozzle are shaped so that the exhaust gases continue to increase their velocity as they

travel out of the engine. Based on the geometry of the nozzle, it can be categorized under co-annular, convergent or convergent-divergent (CD) nozzle.

2.2.2 Types of jet engines

There are many different types of jet engines for aircraft like turbojet, turbofan, turboprop, and turboshaft engines. These, in turn, can be subdivided based on their design and internal arrangement of their components like single compressor engine, dual compressor (twin spool) engines, high bypass ratio engines, and low bypass ratio engines. All of the gas turbine engines like turbofans, turboprops and turboshaft engines work on the same principle as the above described turbojet. As the turbofan being the engine used in this research, a detailed explanation of the gas turbine engine (turbofan) operation is presented in the sections to be followed.

a) Turbojet: A turbojet as shown in Figure 2.4 is a type of aircraft gas turbine engine which uses only the thrust developed within the engine to produce the propulsive forces. These are well suited for high flying, high speed aircraft as they are efficient at high altitude and airspeed. Turbojet aircrafts need long runways for takeoff.

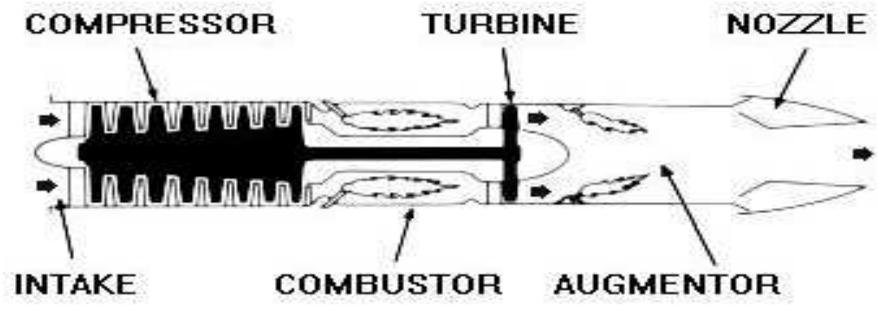

Figure 2.4: Turbojet [9]

b) Turboprop: A turboprop is a turbojet engine with an additional turbine augmented to it to drive a propeller (through a speed reducing gear system). Figure 2.5 shows the schematic of a Turboprop. These engines are also called as propjets. The additional turbine placed in the path of the exhaust gases is called the free turbine. This free turbine is mounted on the shaft that drives the propeller.

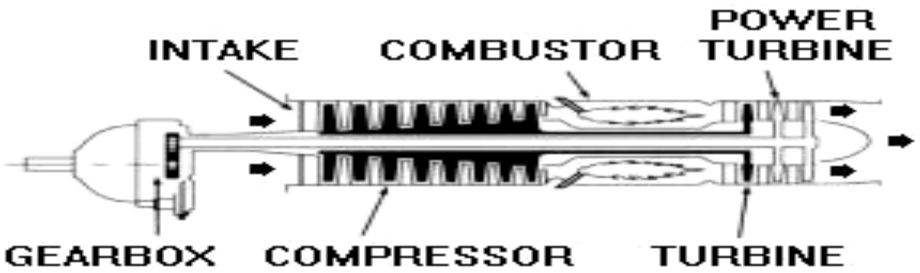

Figure 2.5: Turboprop/ Turboshaft [9]

c) Turboshaft: The turboprop engine in which the shaft of the free turbine is used to drive something other than the propeller is called the turboshaft. The other things that can be driven by the free turbine shaft are rotor of a helicopter, boats, ships, trains and automobiles. The shaft turbine engine is the other name for turboshaft engine.

Both the turboprop and turboshaft engines are more complicated and heavier than the turbojet engine. They produce more thrust at low subsonic speeds. Their propulsive efficiency (output divided by input) decreases as the speed increases, where as it increases in the turbojet case.

d) Turbofan: A turbofan is similar to the turboprop with the gear driven propeller replaced with an axial flow fan with rotating blades and stationary vanes. The schematic

of a turbofan is shown in Figure 2.6. The fan makes a substantial contribution to the total thrust by accelerating the air passing through it. Some amount of the total air entered through the fan that doesn't pass through the engine for burning is called the secondary airflow. The remaining amount of air passing through the engine for burning is called primary airflow. The secondary air flow just passes above the engine and is exhausted in to the outside air through a fan jet-nozzle soon after it leaves the fan or it may be carried backward by an annular fan discharge duct surrounding the engine. The mixing of the fan discharge with exhaust gases from the engine depends on the type of duct used. The short ducts result in nonmixed exhaust. However, using long ducts for the fan discharge results in mixing of the of fan discharge with the exhaust from the basic engine. The ratio of secondary airflow to the primary airflow is called the *bypass ratio*.

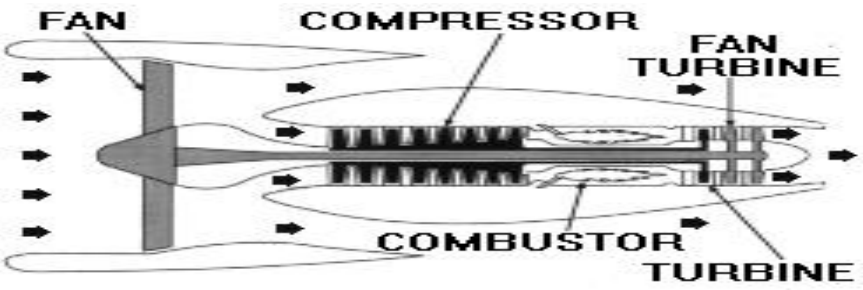

Figure 2.6: Turbofan [9]

The turbofan incorporates the advantages of both the turboprop and turbojet by having the good operating efficiency and high thrust at even high speeds and altitudes. The lighter fan makes the turbofan lighter when compared with the turboprop having a propeller that would be much heavier than a fan. And also, the design of a turbofan is less complex than a turboprop. The other major difference between a turbofan and a turboprop is that the airflow through the fan is controlled by the design of the engine air

inlet duct in such a manner that the velocity of the air through the fan blades is not greatly affected by the speed of the aircraft. This is the reason for turbofan being more efficient than turboprops at higher speeds.

The turbofan has the advantage of lower noise level for the engine exhaust, when compared with the turbojet delivering same thrust as the turbofan. This lower noise level, an important feature in all commercial airports, makes the turbofan better choice than turbojet. For the above described advantages of the turbofans and many other characteristics, they have become the most widely used power plants (engines) for all conventional large aircrafts, both military and commercial.

The turbofan engines can be subdivided based on the type of fan discharge duct used like long duct or short duct, the amount of bypass ratio like high bypass or low bypass.

2.2.3 Jet engines with afterburners

The military aircrafts like fighter jets require extra busts of a speed during takeoff and climb, or for an intercept mission. This extra speed is achieved by an afterburner added to their engine. An additional thrust of 50 percent or more thrust can be achieved with jet engine equipped with an afterburner. The afterburner is also called an *augmentor* because it is nothing but a pipe attached to the rear of an engine instead of a tail pipe and jet nozzle. Only 25 percent of the air entering the fan is passed through the basic engine for combustion, the remaining 75 percent of the air flow is just passed above the engine.

Sometimes it is mixed with the exhaust gases at the jet nozzle as in long duct type jet engines; however it can be used for combustion in the afterburner by injecting the fuel through spray bars. This additional combustion of exhaust gases (mixed with secondary air flow) results in higher velocities delivering additional thrust. The afterburners develop additional thrust at the cost of additional fuel consumption, so the use of an afterburner is profitable only in those aircrafts that may urgently require increased speed for short periods of time or extra power for short takeoff with heavy loads without considering the fuel consumption.

2.3 Engine performance

Apart from the above described components, a turbofan has many other important components which make the engine perform efficiently. Engine has a lot of actuators, sensors and other instruments mounted on each of its components. These instruments measure some critical parameters of the engine that would reveal the engine performance.

2.3.1 Engine rating

Engine ratings for different flights of an aircraft describe the engine performance over a period of time. The thrust, in pounds, which an engine is designed to develop for takeoff, maximum continuous, maximum climb, and maximum cruise is called the engine rating [8]. These ratings are also interpreted in terms of engine pressure ratio (EPR). EPR can be maintained by the Engine's throttle position which regulates the supply of fuel.
Engine ratings are different for military and commercial engines as they are used for different operations. In military aircraft, the urgency of the mission frequently determines

how the engine will be operated. While in commercial or passenger aircraft, the time between the engine overhaul schedules and maximum reliability are of concern, and more conservative engine operation becomes the rule.

2.3.2 Engine maintenance

Jet engines are precision machines composed of many expensive parts. A thorough understanding of the construction and operation of an engine and its components is vital to good jet engine maintenance. The maintenance in jet engine is divided in to two categories: a) preventive maintenance and b) corrective maintenance. The routine inspection of the various engine components, assemblies, and systems come under the preventive maintenance category. Corrective maintenance is the one in which the malfunctions and damaged parts are fixed or replaced as they occur.

Even though the operation manual of the engine described by the manufacturer gives the details of how often to perform maintenance schedules, the engine performance over a period of time is considered for scheduling the above maintenances to enhance the engine's life. It is a well known fact that any machine's performance degrades for the period of time it works. A turbofan engine's performance also deteriorates over time as it is also a kind of machine.

2.3.3 Engine performance deterioration

As described in the previous section, the engine's performance deterioration plays an important role in the engine maintenance schedule. Engine performance deterioration

also reduces the fuel economy of the engine [10]. Just like the life of a living being is affected by its health, the life of a turbofan is also affected by its performance over a period. Engine's performance is also referred by other terms like health or condition. There are many parameters of the engine which would fully describe the engine's health. It would be impossible or rather difficult to consider all the parameters that would add to the engine's health. Hence, only a certain number of parameters are considered which would have a major effect on the engine's health. These parameters are called *health parameters*. Different engines have different set of health parameters.

Engine condition monitoring devices are used to measure most of the health parameters of the engine. However, some of the parameters cannot be measured because of many difficulties like the problem of mounting the device in a particular position, unavailability of devices for measuring certain parameters, getting inaccurate measurements from the devices or due to the complex design of the turbofan engine. Monitoring and evaluating these health parameters by some means would help in good maintenance and also increase the life of engine. Engine health evaluation can also be very helpful in some predictive control techniques.

2.4 Turbofan engine used in this research (MAPSS)

The engine that is being implemented in this research is a high pressure ratio, dual spool, low bypass military type turbofan engine shown in Figure 2.7, with a digital controller. This engine has all of the basic components as discussed previously in Section 2.2. MAPSS, a generic nonlinear, low frequency, transient, high performance model is

implemented as a simulation model for the above military turbofan engine [2]. MAPSS stands for *Modular Aero Propulsion System Simulation*. This engine model is similar to the models used in various areas of intelligent engine control research such as model-based control and nonlinear performance seeking control.

Because of the high complexities in the design and operation of a turbofan engine, it is desirable for the engine models to have a simulation environment that is straightforward, has modular graphical components and has the ability to convert a control design into real-time code. Because of the current technology in advanced modeling software, such as MATLAB [12] and Simulink [13], such an engine model, represented in a graphical simulation environment, has the capability to become an extremely powerful tool in control and diagnostic system development [11].

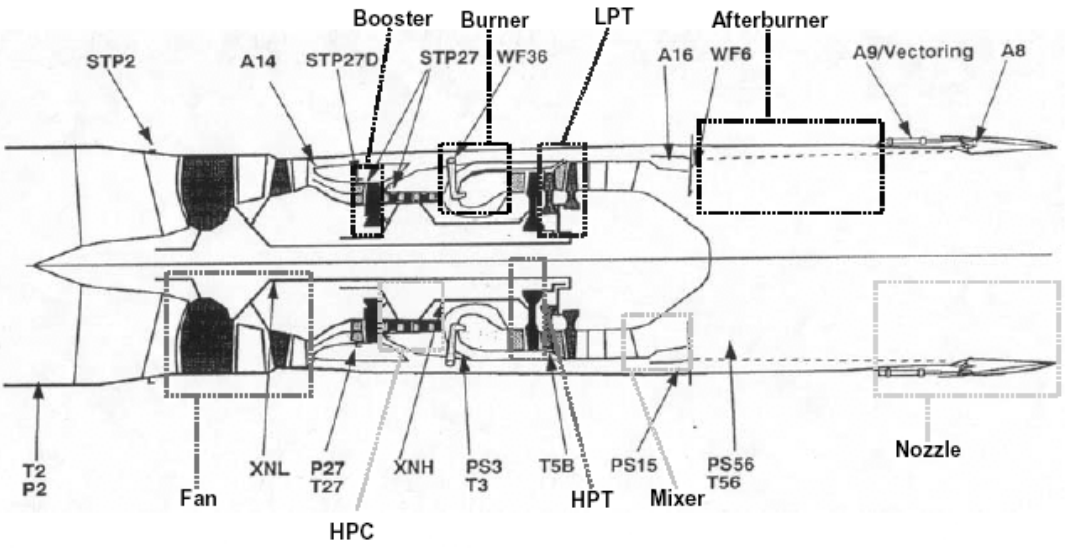

Figure 2.7: Schematic of turbofan engine model [11]

MAPSS is a non real time, nonlinear system composed of the "Controller and Actuator Dynamics" (CAD) and "Component Level Model" (CLM) modules [11]. The computer engine models used in this type of intelligent engine control research are called component level models. The CAD and CLM modules of the MAPSS are managed by a GUI interfaced to them as shown in Figure 2.8. The CLM module in MAPSS environment represents the core engine model with all its components.

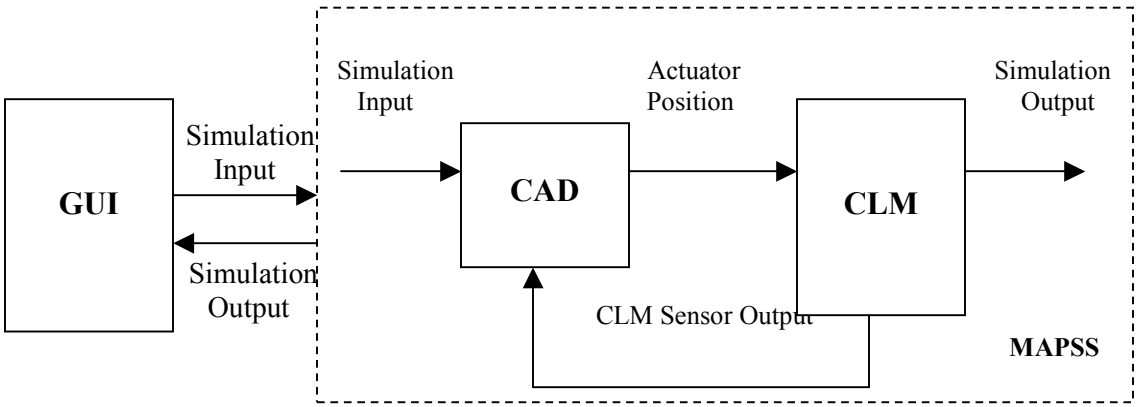

Figure 2.8: MAPSS block diagram (Module interaction) [2]

a) CAD: The CAD module has the engine's controller and actuator dynamics in it. The controller in the CAD module emulates the digital controller for the turbofan engine. This module incorporates all the components or instruments that will be used in the control structure of the engine. The actuator dynamics sub modules are designed based on the mathematical equations of the real time actuators used in the turbofan engines. They simulate instruments like torque motors and servomechanisms for engine components like fan, HPC, booster etc. The actuators and CLM module use the same sampling rate to obtain mass-energy balance inside the components (engine).

b) CLM: The fundamental engine model is represented by the CLM in MAPSS. The CLM has all of the principal components of a turbofan engine like fan, booster, high pressure compressor (HPC), burner, high pressure turbine (HPT), low pressure turbine (LPT), mixer, afterburner (AB), and nozzle as shown in Figure 2.9. The engine components were modeled by mathematical equations before they can be implemented as they have different behaviors like chemical, mechanical, electrical and thermo dynamical which are difficult to implement directly in simulations. There are many subsystems inside each of the component block. These subsystems contain algebraic equations and maps that characterize the behavior of that particular component when simulated. There is no inlet in the CLM typically, because it is not considered to be a part of the engine model. *It is out of the scope of this research to discuss details of all of the algebraic equations involved in an engine model.* The block diagram of the CLM (engine) in MAPSS shown in Figure 2.9 resembles the engine model shown in Figure 2.7 except for the inlet. The overall engine block requires certain iteration steps to ensure a balance of mass flows and energy. The typical parameters like pressure, temperature and flow of certain blocks are implemented as some kind of signals.

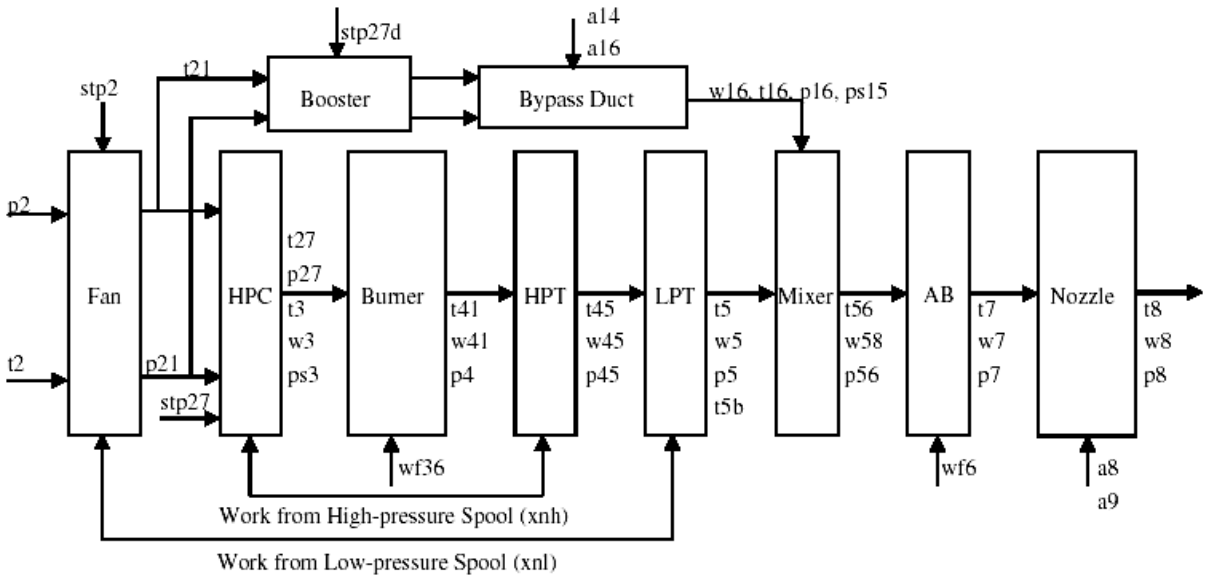

Figure 2.9: CLM with engine components [2]

c) GUI: The GUI block in Figure 2.8 is designed to simplify the user's interaction with the CAD and CLM modules of the MAPSS. The MAPSS graphical user interface designed using Matlab's GUIDE is displayed in Figure 2.10. Apart from the main objective of managing the input/output information of the MAPSS, GUI is also used to simulate the MAPSS model as a whole. The input simulation parameters such as power lever angle (PLA), mach number and altitude of the MAPSS model are given to the system through GUI. PLA is the angle of the throttle in a turbofan engine to produce the required thrust. Mach number is defined as the ratio of the speed of flight to the speed of sound in the same medium. Altitude is the height at which the aircraft is designed to fly. Similarly, the output parameters from the CAD and CLM modules are obtained and displayed through the same GUI panel.

All the components of the engine can be simulated by selecting the components from the simulation block drop down menu in the GUI, and the trend of the

corresponding component parameters can be studied. The entire objects of GUI like the buttons, dropdown menus, text boxes and others have different functions to be performed when activated. The output parameters created by simulating the model, along with user defined input information is stored in an output structure array that will be saved as a MAT-file. This MAT-file can be used for post simulation analysis or to reload certain parameters into the GUI.

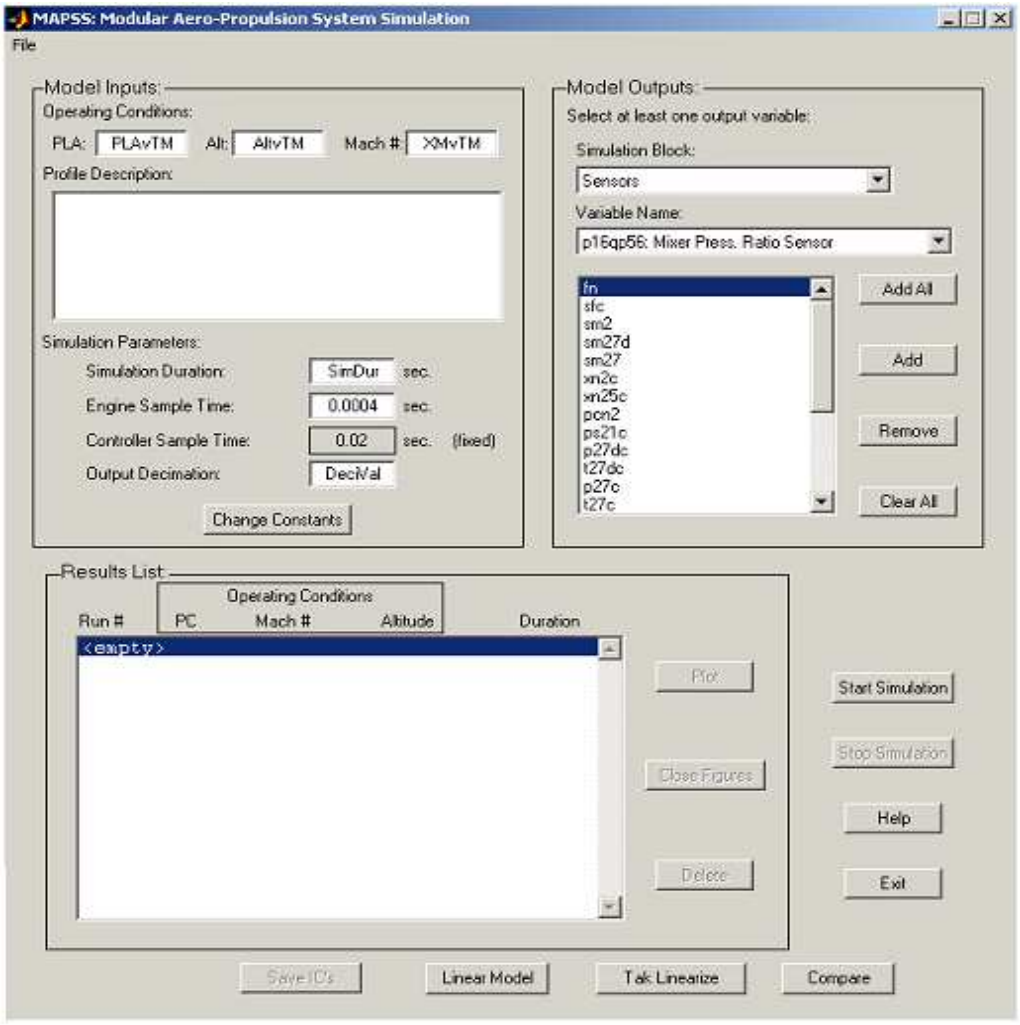

Figure 2.10: MAPSS GUI

2.5 Engine's state space model

Mathematical equations, typically differential or difference equations are used to describe the behavior of processes and to predict their response to certain inputs [14]. These set of equations put in to a common framework is called as the *state space model* of the system. This process of describing the systems by state space models is termed as *modeling.* These models have many useful features like giving an intuitive understanding of the behavior of many dynamical systems and can also be solved efficiently since they are mathematical equations.

$$\dot{x} = f(x,u)$$

$$y = h(x,u) \tag{2.1}$$

Any state space model can be represented with combinations of three parameters of the system as shown in Equation 2.1. These three parameters namely states, inputs and outputs describe the system's behavior as a whole. The inputs and outputs constitute to be the external variables, where as states form the internal variables of the system. The state of a dynamic system is defined as the smallest set of variables such that the knowledge of these variables together with the knowledge of inputs determines the behavior of system at any time.

Similarly, the turbofan engine modeled as MAPSS has a set of states, control inputs and outputs that describe the engine's behavior. The three states of the MAPSS are

1) High pressure rotor speed (xnh)

2) Low pressure rotor speed (xnl)

3) Heat soak temperature (tmpc)

The three control inputs to the model are

1) Main burner fuel flow
2) Variable nozzle area
3) Rear BP door variable area

The eleven sensor outputs of the model are as follows

1) LPT exit pressure
2) LPT exit temperature
3) Percent low pressure spool rotor speed
4) HPC inlet temperature
5) HPC exit temperature
6) Bypass duct pressure
7) Fan exit pressure
8) Booster inlet pressure
9) HPC exit pressure
10) Core rotor speed
11) LPT blade temperature

Apart from the above mentioned parameters there are certain important parameters called health parameters that describe the health of an engine. The importance of these parameters was already discussed in Section 2.3. Estimating these health

parameters over a period of time is the objective of this research. The ten health parameters of the MAPSS model are

1) Fan airflow
2) Fan efficiency
3) Booster tip airflow
4) Booster tip efficiency
5) Booster hub airflow
6) Booster hub efficiency
7) High pressure turbine airflow
8) High pressure turbine efficiency
9) Low pressure turbine airflow
10) Low pressure turbine efficiency

CHAPTER III

LINEAR STATE ESTIMATION

State feedback plays a major role in the control structure of any system. Stability and other desired responses of the system depend on the state feedback given to the system. In practice, the individual state variables of a dynamic system cannot be determined exactly by direct measurements, such as the temperature in the core of a nuclear power plant; instead, the measurements which are functions of state variables are used to estimate the state variables indirectly. It should be noted that these measurements have some random noise associated with them or system by itself might be corrupted with some random noise.

To overcome such problems, estimators are designed based upon known information regarding process (system dymanics) and the noise paramters, to provide a good *estimate* of the states from the noisy mesurement data. Depending on the paramters used with in the estimator, different terms are used to refer the estimation procedure. *Filtering* refers to estimating the state vector at the current time, based upon all past measurements. *Prediction* refers to estimating the state at a future time. *Smoothing* refers

to estimating the value of the state at some prior time, based on all measurements taken up to the current time [15]. The difference between the *estimator's* output and the true state is termed as *estimation error* which is also used as the *cost function* for the estimator. It is obvious to think that the estimation error has to be minimum for the state estimates to be as close as possible to the true states. Thus, an *estimator* which provides the estimates with optimum (minimum) estimation error is called an *optimal state estimator*. Section 3.1 discusses different kinds of estimation techniques, and Section 3.2 describes state estimation in time varying systems. The classical Kalman filter equations are derived in Section 3.3.

3.1 Different estimation techniques

Estimation techniques can be classified based on the criterion of their cost function. For easy understanding of the reader, the estimation of a constant is considered first before discussing the estimation of a time varying vector.

3.1.1 Least squares estimation

Suppose there are n measurements for a same scalar constant x, then intuitively the average (mean) of the n measurements would result in estimate of x . This estimate is optimal in the sense that it minimizes the sum of the squared errors (SSE) between the measurements and the predicted measurements, and is a linear function of the measurements [15].

Consider an n-dimensional constant vector x which is unknown, and a measurement vector z related to the constant vector x obtained from k measurements. Let e be the error in mesurements and H be the observation matrix of $k \times n$ dimension. Then the relation between x and z is given by Equation 3.1 below,

$$z = Hx + e \tag{3.1}$$

Now, if $\hat{x}$ is the estimate of the true state x, then the error between true and estimated state called the *state residual* (ε_x) is given by Equation 3.2a.

$$\varepsilon_x = x - \hat{x} \tag{3.2a}$$

$$\varepsilon_z = z - H\hat{x} \tag{3.2b}$$

Similar to the *state residual,* the error in true measurement and estimated measurements is called the *measurement residual* and is obtained as ε_z in Equation 3.2b.

The cost function represented by J is defined as follows

$$J = \frac{1}{2} E(\varepsilon_z{}^T \varepsilon_z)$$

$$J = \frac{1}{2} E(z^T z - \hat{x}^T H^T z - z^T H\hat{x} + \hat{x}^T H^T H\hat{x}) \tag{3.3}$$

Minimizing J with respect to $\hat{x}$ would result in the best estimate $\hat{x}$ for true state x, i.e., partially differentiating J with respect to $\hat{x}$.

$\frac{\partial J}{\partial \hat{x}} = 0$ results in

$$\hat{x} = (H^T H)^{-1} H^T z \tag{3.4}$$

$$\hat{x} = H^L z$$

where H^L is the left pseudo inverse of H. This exists only when the number of known variables (measurements) is greater than the number of unknowns (states).

3.1.2 Weighted least squares estimation

This kind of estimation is used when there is a weighting function on the errors for different measurements. The weighting function was identical for all the measurements in the previous section, where all measurements were obtained with error statistics. Weighting functions are assigned to the error vectors when measurements were obtained with different error statistics, i.e., when we have more confidence in some measurements than others. The cost function for weighted least squares estimator can be derived by incorporating this additional information about the errors weighting function.

Consider the same vector x as in Equation 3.1, with weighting functions for the error vector as follows.

$$\begin{aligned} E(e_1^2) &= \sigma_1^2 \\ &\vdots \\ E(e_k^2) &= \sigma_k^2 \end{aligned} \tag{3.5}$$

The cost function J is defined to be the quadratic cost function of a normalized measurement residual as in the following Equation 3.5 [16].

$$J = \frac{1}{2} E(\varepsilon_z{}^T N^{-T} N^{-1} \varepsilon_z) \tag{3.6}$$

where N is the k x k diagonal matrix defined as $N = \begin{bmatrix} \sigma_1 & \cdots & 0 \\ \vdots & \ddots & \vdots \\ 0 & \cdots & \sigma_k \end{bmatrix}$

Minimizing the cost function J would result in the best estimate $\hat{x}$ as

$$\hat{x} = (H^T S^{-1} H)^{-1} H^T S^{-1} z \tag{3.7}$$

where $S \equiv N^T N$

3.1.3 Bayesian estimation

Least squares estimation being a deterministic approach can only be used in the case where there is no probabilistic description for either the unknown to be estimated or the measurements considered. However, the *maximum likelihood* philosophy is used when the *x* and *z* are assigned with some probability density functions. In this approach the estimate $\hat{x}$ will take that value which maximizes the probability of the measurements *z* that actually occurred, taking into account known statistical properties of *e* [15].

Considering the same example as in Equation 3.1, the conditional probability density function for *z,* conditioned on a given value for *x,* is just the density for *e* centered around *Hx*. Considering *e* to be a zero mean, Gaussian distributed observation with covariance matrix *R*, we get

$$p(z \mid x) = \frac{1}{(2\pi)^{1/2} \mid R \mid^{1/2}} \exp\left[-\frac{1}{2} (z - Hx)^T R^{-1} (z - Hx) \right] \tag{3.8}$$

The objective of maximizing this probability of measurements is done by minimizing the exponent in brackets. Minimizing this exponent is similar to minimizing the cost function in Equation 3.6, with *R* replacing the $N^T N$ matrix, i.e., interpreting the noise vector with its probabilistic covariance. Hence, the estimate would be the same result as obtained in Equation 3.7, but with *S* replaced by *R*.

$$\hat{x} = (H^T R^{-1} H)^{-1} H^T R^{-1} z \tag{3.9}$$

Bayesian estimation, developed by applying Bayes' theorem to the above maximum likelihood approach, is used when the statistics (probability density function) of x is also known along with the statistics of the measurements z. Any estimation algorithm is implemented to find the best estimate from the given measurements. This is nothing but finding the conditional probability density function of x given the statistics of z, i.e., $p(x|z)$, which can be evaluated using Bayes' theorem as

$$p(x \mid z) = \frac{p(z \mid x) p(x)}{p(z)} \tag{3.10}$$

where $p(x)$ is the a priori probability density function of x and $p(z)$ is the probability density function of the measurements. Depending upon the criterion of optimality, an estimate of x can be computed from $p(x|z)$.

3.1.4 Recursive least squares estimation

The previously discussed estimators are for the time invariant case. If the measurements are taken at several time steps, then the above methods can be implemented by augmenting the newly available measurements to the old ones. But it would be difficult to store all the measurement sets. However, to overcome this difficulty, the prior estimate can be used as the starting point for a sequential estimation algorithm that assigns proper relative weighting to the old and new data [16]. This sequential estimation algorithm is called a *recursive filter*; where there is no need to store past measurements for the purpose of computing present estimates.

Scalar case

Before going for the estimation of a constant vector, the recursive estimation technique is described for a scalar constant similar to the previous cases. Let us consider the following problem of estimating a scalar constant x based on k noise-corrupted measurements.

$$z_i = x + e_i \tag{3.11}$$

where $i=1,2...k$ and e_i is considered to be a white noise sequence.

An unbiased, minimum variance estimate $\hat{x}_k$ would be the average or mean of the measurements

$$\hat{x}_k = \frac{1}{k}\sum_{i=1}^{k} z_i \tag{3.12}$$

When there is an additional measurement available, the new estimate incorporates that new measurement by changing the above average with addition of new measurement as shown below

$$\hat{x}_{k+1} = \frac{1}{k+1}\sum_{i=1}^{k+1} z_i$$

The above equation can be manipulated to show the importance of the prior estimate $\hat{x}_k$ as follows.

$$\hat{x}_{k+1} = \frac{1}{k+1}\left(\frac{1}{k}\sum_{i=1}^{k} z_i\right) + \frac{1}{k+1} z_{k+1} = \frac{k}{k+1}\hat{x}_k + \frac{1}{k+1} z_{k+1}$$

This can be termed as a recursive linear estimator by manipulating the above equation as follows.

$$\hat{x}_{k+1} = \hat{x}_k + \frac{1}{k+1}(z_{k+1} - \hat{x}_k) \tag{3.13}$$

The new estimate obtained in Equation 3.13 is given by the prior estimate plus an appropriately weighted difference between the new measurement and its expected value, given by the prior estimate [15]. This weighting factor for the measurement residual is called the *estimator gain*.

Vector case

Consider the same vector *x* as in Equation 3.1, with time varying case, i.e., with different sets of measurements at different time steps, represented by the following equations.

$$z_k = H_k x + e_k \tag{3.14}$$

where *x* is the constant unknown vector to be estimated, z_k is the measurement vector with H_k as the observation matrix obtained at *k*-th time step and e_k as the corresponding measurement noise (error) vector.

From Equation 3.13, we can evaluate the estimate at present time as

$$\hat{x}_k = \hat{x}_{k-1} + K_k(z_k - H_k \hat{x}_{k-1}) \tag{3.15}$$

where K_k is the estimator gain, and $(z_k - H_k \hat{x}_{k-1})$ is termed as the correction term (measurement residual).

Finding the unknown estimator gain was simple in the scalar case. But, for a time varying case, this calculation is little cumbersome with a lot of math. Considering the fact that estimation error should be minimum for any optimal estimator, the first two moments

(probabilistic) of the estimation error are utilized to calculate the estimator gain. The expected value or mean of the estimation error being the first moment can be calculated as

$$
\begin{aligned}
E(\varepsilon_{x,k}) &= E(x - \hat{x}_k) \\
&= E(x - \hat{x}_{k-1} - K_k(z_k - H_k\hat{x}_{k-1})) \\
&= E(x - \hat{x}_{k-1}) - K_k E(H_k x + e_k - H_k\hat{x}_{k-1}) \\
&= (I - K_k H_k)E(\varepsilon_{x,k-1}) - K_k E(e_k) \qquad (3.16)
\end{aligned}
$$

$E(\varepsilon_{x,k})$ can be 0 if $E(e_k) = 0$ and also $E(\varepsilon_{x,k-1}) = 0$. These conditions can be obtained by assuming the measurement noise (e_k) to be zero mean and the average estimation error to be zero. The estimate obtained with these conditions is an *unbiased estimate* since the expected value of the estimate is equal to the expected value of the true state.

Now using the second moment, which is the covariance of the estimation error, the cost function of the estimator is defined. The estimation error covariance, P_k is defined as

$$
\begin{aligned}
P_k &\equiv E(\varepsilon_{x,k}\varepsilon_{x,k}^T) \\
&= E\{[(I - K_k H_k)E(\varepsilon_{x,k-1}) - K_k E(e_k)][...]^T\} \\
&= (I - K_k H_k)P_{k-1}(I - K_k H_k)^T + K_k R_k K_k^T \qquad (3.17)
\end{aligned}
$$

where R_k is the measurement noise covariance ($E(e_k e_k{}^T)$)

The cost function of the recursive estimator is a modified form of the least squares estimator's cost function, in the sense of incorporation of the covariance of the estimation error.

$$J = \frac{1}{2} E(\varepsilon_{x,k}{}^T \varepsilon_{x,k})$$

$$= \frac{1}{2} \mathrm{Tr}\{\mathrm{E}(\varepsilon_{x,k} \varepsilon_{x,k}{}^T)\} \qquad \text{where } Tr \text{ represents the trace of a matrix}$$

$$= \frac{1}{2} \mathrm{Tr}(P_k)$$

substituting P_k from Equation 3.17,

$$J = \frac{1}{2} \mathrm{Tr}[(I - K_k H_k) P_{k-1} (I - K_k H_k)^T + K_k R_k K_k{}^T] \tag{3.18}$$

Minimizing this cost function with respect to the estimator gain and equating it to minimum (zero) would give the value of the optimal estimator gain, i.e.,

$$\frac{\partial J}{\partial K_K} = \frac{1}{2}[2(I - K_k H_k) P_{k-1} (-H_k)^T + 2K_k R_k]$$

then, making $\frac{\partial J}{\partial K_K} = 0$, would result in the optimal estimator gain K_k as in Equation 3.19, by using the lemma $\frac{\partial \mathrm{Tr}(ABA^T)}{\partial A} = 2AB$.

$$K_k = P_{k-1} H_k{}^T (H_k P_{k-1} H_k{}^T + R_k)^{-1} \tag{3.19}$$

Though Equations 3.17 and 3.19 represent the estimator error covariance and estimator gain, these are not the only derived equations that represent those values. There may be other equations derived for these terms, but they can also be obtained by math manipulations from the above equations.

3.2 State estimation in a linear system

Estimation of a constant vector was only discussed in the previous sections and those estimation techniques can also be implemented for estimating the states of a dynamic system. But since the estimated quantities may not be constant, the estimator would tend to ignore information contained in the later measurements [16]. Hence, the estimator should incorporate the additional information like the dynamic effects of the system model and its inputs on the estimate ($\hat{x}_k$) and its uncertainty, i.e., estimation error covariance (P_k). The inputs and initial conditions of a dynamic system are random, due to which the state itself must be considered a random variable. This is where the estimation is effected by the probabilistic functions of the variables. The propagation of the state and its uncertainty through the time history, interpreted with the probabilistic approach is explained for a discrete time linear time varying system in the following example.

Consider a linear discrete time varying system as described by the following equation

$$x_k = A_{k-1}x_{k-1} + B_{k-1}u_{k-1} + \Lambda_{k-1}w_{k-1} \tag{3.20}$$

where u_{k-1} is the known input to the system, w_{k-1} is the white noise with zero mean and covariance Q_{k-1}, i.e., $w_k \sim N(0, Q_k)$. The initial condition of the state (x_0) is a Gaussian random variable with its mean value and covariance matrix as

$$E(x_0) = m_0$$

$$E[(x_0 - m_0)(x_0 - m_0)^T] = P_0 \tag{3.21}$$

It is necessary to propagate the mean and covariance of the state, to estimate the state for the total time history of the system. The mean of the state is propagated through the time according to the following equations

$$E(x_k) = E(A_{k-1}x_{k-1} + B_{k-1}u_{k-1} + \Lambda_{k-1}w_{k-1})$$

$$= A_{k-1}m_{k-1} + B_{k-1}u_{k-1} \tag{3.22}$$

since we have $E(w_{k-1}) = 0$ and $E(u_{k-1}) = u_{k-1}$ from the assumptions made previously. Similarly consider the propagation of covariance (uncertainty) as described below.

$$P_k \equiv E[(x_k - m_k)(x_k - m_k)^T]$$

Using Equation 3.22 we obtain

$$(x_k - m_k)(x_k - m_k)^T = [A_{k-1}(x_{k-1} - m_{k-1}) + B_{k-1}(0) + \Lambda_{k-1}w_{k-1}][...]^T$$

$$P_k = E\{[A_{k-1}(x_{k-1} - m_{k-1}) + \Lambda_{k-1}w_{k-1}][A_{k-1}(x_{k-1} - m_{k-1}) + \Lambda_{k-1}w_{k-1}]^T\}$$

$$= E\{A_{k-1}(x_{k-1} - m_{k-1})(x_{k-1} - m_{k-1})^T A_{k-1}^T + A_{k-1}w_{k-1}w_{k-1}^T A_{k-1}^T + A_{k-1}(x_{k-1} - m_{k-1})w_{k-1}^T \Lambda_{k-1}^T + A_{k-1}w_{k-1}(x_{k-1} - m_{k-1})^T A_{k-1}^T\}$$

since $E(w_{k-1}w_{k-1}^T) = Q_{k-1}$ and $E(w_{k-1}x_{k-1}^T) = 0$ we get

$$P_k = A_{k-1} P_{k-1} A_{k-1}^T + \Lambda_{k-1} Q_{k-1} \Lambda_{k-1}^T \tag{3.23}$$

Equations 3.22 and 3.23 are very important because they describe the propagation of the state and its estimation error covariance through the time history of the system.

Recursive estimation techniques which are implemented for estimating the states of the dynamic system using the above propagations result in different kinds of filters and predictors to be discussed in the next section.

3.3 Discrete time Kalman filter

The systems considered in the previously described estimation algorithms were just measurement systems. This section would discuss the state estimation of the system by considering the state estimate propagation as described by the system state equations (Section 3.2) and then updating estimates recursively by using the system's measurement equations (Section 3.1.4). In 1960, R.E. Kalman published his famous paper describing a recursive solution to the discrete-data linear filtering problem. He formulated and solved the filtering problem for gauss-markov sequences through use of state-space representation and the viewpoint of conditional distributions and expectations [17].

The purpose of a filter is to compute the state estimate $\hat{x}_k$, while an optimal filter minimizes the spread of the estimation-error probability density in the process [16] which means minimizing the mean square estimation error. A recursive optimal filter propagates the conditional probability density function from one sampling instant to the next, taking into account system dynamics and inputs, and it incorporates measurements and

measurement error statistics in the estimate [16]. As discussed in the previous section, the state estimate $\hat{x}_k$ is specified by expected value (*mean*) of the true state's (x_k) conditional probability density function and the spread of uncertainty in estimate is specified as the *covariance* matrix. This recursive generation of the mean and covariance in finite time can be explained in the following five steps:

1) State Estimate Extrapolation (Time Propagation)

2) Covariance Estimate Extrapolation (Time Propagation)

3) Filter Gain Computation

4) State Estimate Measurement Update

5) Covariance Estimate Measurement Update

The first two steps that describe the propagation of the estimate (mean) of the state and its uncertainty (estimation error covariance) are already discussed in the previous section of (Section 3.2). The last three steps can be performed by the recursive (weighted) least squares estimation technique as discussed in that Section 3.1.4.

The mathematical form of the five steps performed in the Kalman filter can be derived by considering a linear time varying discrete time stochastic system represented by Equation 3.24a and 3.24b.

$$x_k = A_{k-1}x_{k-1} + B_{k-1}u_{k-1} + \Lambda_{k-1}w_{k-1} \tag{3.24a}$$

$$z_k = C_k x_k + n_k \tag{3.24b}$$

Equation 3.24a represents the state equation of the system with *x* as the state vector, *u* as the control input to the system and *w* as the process noise in the system. This process noise is considered to be a zero-mean white noise, Gaussian random variable with Q_k as its covariance.

$$E(w_k) = 0$$

$$E(w_k w_k^T) = Q_k \tag{3.25}$$

Equation 3.24b describes the measurement model of the system. *z,* the measurement vector, is a combination of states *x* associated with some measurement noise represented by *n.* Similar to the process noise, this noise *n* is also a zero-mean white noise, Gaussian random variable with R_k as its covariance.

$$E(n_k) = 0$$

$$E(n_k n_k^T) = R_k \tag{3.26}$$

The system matrices represented by *A*, *B, C*, and Λ are considered to be known. The important assumption to be considered is that the process noise and measurement noise are independent, i.e., there is no correlation existing between them.

$$E(n_k w_k^T) = E(w_k n_k^T) = 0 \tag{3.27}$$

It is also assumed that values of the initial state estimate $\hat{x}_0$ and initial estimation error covariance P_0 are known beforehand as discussed in Section 3.2.

$$\hat{x}_0 = E(x_0) \quad \text{and} \quad P_0 = E[(x_0 - \hat{x}_0)(x_0 - \hat{x}_0)^T]$$

There are two main transitions to be considered for the propagation of any variable of the system through the time instants. They are state update and measurement update (transition). Figure 3.1 describes these transitions in a more simple way.

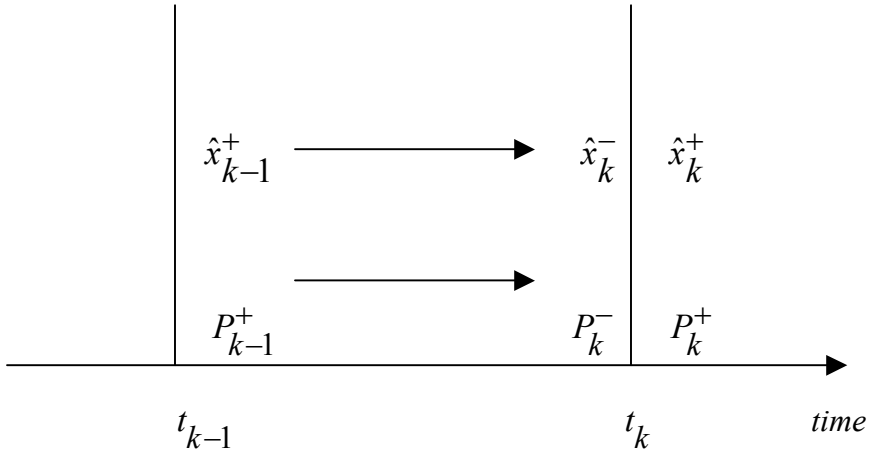

Figure 3.1: Mean and covariance propagation

In Figure 3.1, the superscripts (–) represent the state estimate and covariance before the measurement is processed at time instant (k) and the superscripts (+) represent their corresponding values after the measurement is processed.

The Kalman filter equations were derived by implementing the results of the previous sections to the system described in Equation 3.24.

Time update

The first step of propagating the state estimate is derived by using Equation 3.22 in Section 3.2.

$$\hat{x}^-_k = A_{k-1}\hat{x}^+_{k-1} + B_{k-1}u_{k-1} \tag{3.28}$$

Similar to the above step, estimation error covariance is propagated with time according to the Equation 3.23 in Section 3.2.

$$P_k^- = A_{k-1} P_{k-1}^+ A_{k-1}^T + \Lambda_{k-1} Q_{k-1} \Lambda_{k-1}^T \tag{3.29}$$

Measurement update

Now that $\hat{x}_k^-$ is calculated, $\hat{x}_k^+$ (which is the state estimate obtained after the measurement update) is calculated using the RLS estimation technique as discussed in Section 3.1.4.

We calculate the Kalman gain from Equation 3.19, but in this case P_{k-1} is replaced by P_k^- which represents the estimation error covariance before the measurements are obtained.

$$K_k = P_k^- C_k^T [C_k P_k^- C_k^T + R_k]^{-1} \tag{3.30}$$

Using the above Kalman gain, the state estimate and estimate error covariance are updated after processing the measurements as discussed in Section 3.1.4. But in this case $\hat{x}_{k-1}$ is replaced by $\hat{x}_k^-$, P_{k-1} is replaced by P_k^-, $\hat{x}_k$ is replaced by $\hat{x}_k^+$ and P_k is replaced by P_k^+ in the Equations 3.15 and 3.17.

$$\hat{x}_k^+ = \hat{x}_k^- + K_k (z_k - C_k \hat{x}_k^-) \tag{3.31}$$

$$P_k^+ = (I - K_k C_k) P_k^- (I - K_k C_k)^T + K_k R_k K_k^T \tag{3.32}$$

The last five equations represent the fundamental Kalman filter equations; however there are different forms for these KF equations which are obtained by manipulating the above equations with some linear algebra. The important property of the Kalman filter is that it's a linear filter and it can estimate the states of a linear system only. However, it can be extended to a nonlinear system by linearizing the system which will be discussed in Chapter IV. The Kalman filter is considered to be the best linear filter in estimating the states of a system with both process and measurement noise, i.e., *w* and *n*, are uncorrelated and white. The quantity $(z_k - C_k \hat{x}_k^-)$ used to update the state estimate in Equation 3.31 is called the *innovations*. The same concept can be extended to continuous time systems too. Many other filters are designed based on these basic Kalman filter equations, like

1) Steady state KF

2) Constrained KF

3) Robust KF

4) Square root KF

5) Sequential KF

These filters work similar to the fundamental Kalman filter. In the steady state KF a steady state gain is used for propagating the estimate and its error covariance through time. A Kalman filter designed with certain constraints on the estimates is called the constrained KF [10]. The robust KF addresses uncertainties in the process and measurement noise covariances and gives better results than the standard Kalman filter [19]. Similarly, the other Kalman filters incorporate certain other factors in estimating the states.

CHAPTER IV

LINEARIZED KALMAN FILTER

The estimation techniques discussed in the previous chapter can only be applied to linear systems. However, most physical systems encountered in nature are nonlinear systems. For several reasons, the problem of filtering and smoothing for nonlinear systems is considerably more difficult and admits a wider variety of solutions than does the linear estimation problem [15]. This difficulty arises because of the nonlinear elements in the systems which alter the probability density function of signals and noise as they are transmitted through the time, i.e., Gaussian inputs cause non-Gaussian response. The shapes of the distributions change when probability density functions are transmitted through nonlinear elements. Fortunately, estimators for many nonlinear systems can be derived based on basic Kalman filter as stated in the previous chapter; though not precisely "optimum", they are "optimal" in the sense that they tend to the optimum. Section 4.1 discusses nonlinear estimation along with different nonlinear estimation techniques. Linearization process and different linearization techniques are explained in Section 4.2. Sections 4.3 and 4.4 discuss linearization and discretization of the turbofan

engine model (MAPSS) used in this research. An alternate equivalent Kalman filter (*a priori*) equations are derived in Section 4.5. Finally, Section 4.6 discusses the graphical user interface developed for the turbofan health parameter estimation.

4.1 Nonlinear estimation

The basic design of any (recursive) filter is based on the propagation of the state estimate and its error covariance through the system. In linear systems, the state estimate which is a GRV (Gaussian random variable) is transmitted linearly but transmitting the Gaussian through nonlinear elements doesn't give the same shape of the distribution. There are basically two types of propagations of mean and variance through nonlinear systems. The first type involves propagating the state estimate analytically through the first order linearization of the nonlinear system. Linearized Kalman filter, extended Kalman filter and hybrid extended Kalman filter use this type of propagation. The second type involves approximating the state distribution by a small set of carefully chosen sample points and then propagating these sample points through the true nonlinear system. Unscented Kalman filter, a new nonlinear estimation algorithm, is the result of the second type of propagation. UKF is discussed in detail in the Chapter VI.

4.1.1 Linearized Kalman filter

Linearized Kalman filter and extended Kalman filter are mainly based on the linearization of the systems which will be discussed in the Section 4.2. Consider a nonlinear system described by the following equations.

$$\dot{x} = f(x,u,w,t)$$

$$z = h(x,t) + n(t) \tag{4.1}$$

where x is the state vector, u is the control input vector and z is the measurement vector. Similar to the linear case discussed in Section 3.3, w and n are the process and measurement noise which have zero mean and covariances Q and R respectively.

The nonlinear system represented by Equation 4.1 can be approximated by a linear system by applying the Taylor's series expansion to the equation. The linearized Kalman filter linearizes the system about the nominal trajectory, considering the nominal values of state variables and control inputs to be fairly well known beforehand. Hence, it is obvious that a linearized Kalman filter can be implemented only when the nominal trajectory of the system is well known.

$$\dot{x} \approx f(x_0,u_0,w_0,t) + \left.\frac{\partial f}{\partial x}\right|_0 (x - x_0) + \left.\frac{\partial f}{\partial u}\right|_0 (u - u_0) + \left.\frac{\partial f}{\partial w}\right|_0 (w - w_0)$$

$$z \approx h(x_0,t) + \left.\frac{\partial h}{\partial x}\right|_0 (x - x_0) + n(t) \tag{4.2}$$

$\left.\frac{\partial ..}{\partial ..}\right|_0$ represents the corresponding partial derivative evaluated at (x_0,u_0,w_0) i.e., nominal values which are well known. These partial derivatives which represent the system matrices are called the *Jacobians*.

Taylor's series expansion of the nonlinear equations approximated as the linear equations can be represented as following, by denoting the Jacobians as $F = \frac{\partial f}{\partial x}, G = \frac{\partial f}{\partial u}, L = \frac{\partial f}{\partial w}, H = \frac{\partial f}{\partial x}$.

$$\dot{x} = f(x_0, u_0, w_0, t) + F(x - x_0) + G(u - u_0) + L(w - w_0)$$

$$z = h(x_0, t) + H(x - x_0) + n(t)$$

Assuming $\dot{x}_0 = f(x_0, u_0, w_0, t)$, $z_0 = h(x_0, t)$ and $w_0 = 0$ which are priorly known and using the equations $x - x_0 = \Delta x$, $u - u_0 = \Delta u$, $w - w_0 = \Delta w = w$, $\dot{x} - \dot{x}_0 = \Delta \dot{x}$ and $z - z_0 = \Delta z$, the nonlinear system can be approximated by a linear system as

$$\Delta \dot{x} = F \Delta x + G \Delta u + Lw$$

$$\Delta z = H \Delta x + n \tag{4.3}$$

The standard Kalman filter can be applied to the above linear system and the change in states ($\Delta \hat{x}$) can be estimated as

$$\Delta \dot{\hat{x}} = F \Delta \hat{x} + G \Delta u + K(\Delta z - H \Delta \hat{x}) \tag{4.4}$$

$$K = PH^T R^{-1} \tag{4.5}$$

$$\dot{P} = FP + PF^T + LQL^T - PH^T R^{-1} HP \tag{4.6}$$

The estimate of the true state can be calculated by adding the estimated change in states to the nominal states as

$$\hat{x} = x_0 + \Delta\hat{x} \tag{4.7}$$

The linearized Kalman filter doesn't give exact optimal estimates, but they would be near to the optimum values, i.e., an approximate optimal estimate, as they are based on the nominal trajectory. This filter would result in more accurate estimates if the changes or perturbations in the control input (Δu) and measurement residual ($\Delta z - H\Delta\hat{x}$) are kept small. This linearized Kalman filtering technique was implemented in this research (thesis) to estimate the health parameters of a turbofan engine (MAPSS).

4.1.2 Extended Kalman filter

The extended Kalman filter results in an improved state estimate with no prior knowledge of a nominal trajectory. This EKF technique is similar to the linearized Kalman filter technique but with different Jacobians. The Jacobians in EKF are not evaluated around the nominal values but they are evaluated around the best estimate obtained at that instant. The extended Kalman filter is called extended Kalman-Bucy filter when the nominal process noise is zero ($w_0 = 0$). The extended Kalman filter retains the linear calculation of the covariance and gain matrices, and it updates the state estimate using a linear function of a filter residual; however it uses the original nonlinear equations for state propagation and definition of the output vector.

Consider the same system as in Section 4.1.1 with some changes in the initial conditions like choosing $x_0 = \hat{x}$ so that $\Delta\hat{x} = 0$ and assuming that u is known so that $\Delta u = 0$

Combining the $\Delta\dot{\hat{x}}$ equation with the $\dot{x}_0$ equation

$$\dot{x}_0 + \Delta\dot{\hat{x}} = f(x_0, u_0, w_0, t) + F\Delta\hat{x} + G\Delta u + K(\Delta z - H\Delta\hat{x}) \tag{4.8}$$

Now by substituting the assumed initial conditions in the above equation, the estimate of the state can be obtained from the following equations

$$\dot{\hat{x}} = f(\hat{x}, u, w_0, t) + K(z - h(\hat{x}, t)) \tag{4.9}$$

$$K = PH^T R^{-1} \tag{4.10}$$

$$\dot{P} = FP + PF^T + LQL^T - PH^T R^{-1} HP \tag{4.11}$$

The hybrid extended Kalman filter is another nonlinear estimation technique used to estimate the states of a continuous nonlinear system with discrete time measurements. All of the nonlinear estimation techniques discussed so far are based on the first order linearization (Taylor series expansion). Different kinds of linearization techniques will be discussed in Section 4.2. The estimates obtained by these techniques are not optimally accurate because it is obvious that there can be errors due to the linearization process. The accuracy of the state estimation can be improved by increasing the order of linearization by using second or higher order linearization. The main limitations of the linearized or extended Kalman filter is that it is difficult to implement and reliable only for systems that are almost linear on the time scale of the updates. The unscented Kalman filter, to be discussed in the Chapter VI, was developed to overcome these limitations.

4.2 Linearization

Linearization is the process of modeling a nonlinear system as a linear system. The linear model is an idealized or simplified version of the more accurate (but more complicated) nonlinear model. The linear mathematical model can then be used in the many analysis and design tools that require a linear model. The linear model accurately represents the dynamics of the nonlinear system at certain operating conditions, but may not be accurate at other operating conditions.

In control engineering, the normal operation of the system may be around an equilibrium point, and the system signals can be considered small deviations around the equilibrium. In this case, it can be useful to approximate the nonlinear system with a linear system. The linear model is approximately equivalent to the nonlinear system if the operating range remains near the linearization point. Linearized models are very important in control engineering. In general, there are many more tools for applying control and estimation techniques to linear systems than there are for nonlinear systems. There are different linearization techniques that can be performed on nonlinear systems. Almost all the linearization techniques are based on Taylor series expansions. The linearization methods that are explored in this chapter (section) are listed below

1) Matlab Linearization
2) Perturbation Linearization
3) Steady State Error Reduction

The accuracy of these linearization methods relative to MAPSS model fidelity and turbofan engine health parameter estimation is investigated.

4.2.1 Matlab Linearization

A nonlinear model can be linearized directly using MATLAB [12] functions such as *linmod*, *dlinmod* and *linmod2*. The equilibrium or operating point is calculated by using MATLAB's *trim* function. The *trim* function finds out the equilibrium point at which the system is at steady state; i.e., the state derivatives are zero. If there is no point at which the system is at steady state, then the *trim* function will give the point at which the state derivative is nearest to 0. MATLAB's *trim* function is invoked as follows.

$$[x, u, y] = trim('sys', x0, u0, y0) \tag{4.12}$$

where x, u, and y are the output equilibrium points for the system described by '*sys*,' and $x0$, $u0$, and $y0$ are the user's initial guess for the equilibrium points.

The *linmod* function obtains a linear model from a system of ordinary differential equations that are implemented as a Simulink [13] model. The *dlinmod* function can linearize discrete, multirate, and hybrid continuous-time and discrete-time systems at any given sampling time. This is usually used for linearizing discrete-time systems. The *linmod* function is invoked as follows.

$$[A, B, C, D] = linmod('sys', x, u) \tag{4.13}$$

where x and u are the outputs of the *trim* function. This gives the linearized model of system '*sys*' (in A, B, C, and D matrices) around the specified operating point.

4.2.2 Perturbation Linearization

A nonlinear system can be represented by the following state space equations.

$$\dot{x} = f(x,u,t)$$

$$y = h(x,u,t) \tag{4.14}$$

where f and h are nonlinear functions, x is the state vector, u is the control vector, and y is the output vector. The nonlinear system is run in closed loop until it reaches steady state (i.e., $\dot{x}$=0). Once the system reaches steady state, the resulting state vector $x0$, input vector $u0$, and output vector $y0$ are saved as the nominal values.

4.2.2a Linearization with respect to states

Each state is perturbed individually, and the corresponding changes in the state derivatives and output vectors are calculated. The nonlinear system represented by Equation 4.14 can be linearized to the system described by following equations.

$$\begin{aligned} \Delta\dot{x} &= A\Delta x + B\Delta u \\ \Delta y &= C\Delta x + D\Delta u \end{aligned} \tag{4.15}$$

where columns of the A and C matrices are calculated by using the following equations.

$$\Delta x_i = \text{change in } i^{th} \text{ element of } x \text{ vector}$$

$$\Delta\dot{x}_1 = \text{change in } \dot{x} \text{ vector due to change in } x_1 \text{ (at the initial time)}$$
$$\vdots \qquad\qquad \vdots$$
$$\Delta\dot{x}_n = \text{change in } \dot{x} \text{ vector due to change in } x_n \text{ (at the initial time)}$$

$$[\Delta\dot{x}_1 \quad \cdots \quad \Delta\dot{x}_n] = A \begin{bmatrix} \Delta x_1 & 0 & 0 \cdots\cdots 0 \\ 0 & \Delta x_2 & \vdots \\ \vdots & & \ddots \quad \vdots \\ 0 & \cdots\cdots\cdots\cdots & \Delta x_n \end{bmatrix}$$

$$= \begin{bmatrix} A_{11} \cdots\cdots\cdots A_{1n} \\ \vdots \qquad\qquad \vdots \\ \vdots \qquad\qquad \vdots \\ A_{n1} \cdots\cdots\cdots A_{nn} \end{bmatrix} \begin{bmatrix} \Delta x_1 & 0 & 0 \cdots\cdots 0 \\ 0 & \Delta x_2 & \vdots \\ \vdots & \ddots & \vdots \\ 0 & \cdots\cdots\cdots\cdots & \Delta x_n \end{bmatrix}$$

$$= \begin{bmatrix} A_{11}\Delta x_1 & \cdots\cdots & A_{1n}\Delta x_n \\ \vdots & & \vdots \\ \vdots & & \vdots \\ A_{n1}\Delta x_1 & \cdots\cdots & A_{nn}\Delta x_n \end{bmatrix}$$

$$\Delta \dot{x}_1 = (1^{st} \text{ column of } A) \times \Delta x_1$$
$$\vdots \qquad\qquad \vdots$$
$$\Delta \dot{x}_n = (n^{th} \text{ column of } A) \times \Delta x_n$$

$$i^{th} \text{ column of } A = \Delta \dot{x}_i / \Delta x_i$$

The i^{th} columns of the A and C matrices are computed as follows.

$$\begin{aligned} A(:,i) &= (\dot{x} - \dot{x}0)/(x(i) - x0(i)) \\ C(:,i) &= (y - y0)/(x(i) - x0(i)) \end{aligned} \tag{4.16}$$

this is performed for $i = 1, \ldots, n$ where n is the number of states of the system.

4.2.2b Linearization with respect to control inputs

Similar to linearization with respect to states in Section 4.2.2a, the control inputs are perturbed individually and the corresponding changes in the state derivatives and output vectors are calculated. Then the i^{th} column of the B and D matrices are calculated as follows.

$$\begin{aligned} B(:,i) &= (\dot{x} - \dot{x}0)/(u(i) - u0(i)) \\ D(:,i) &= (y - y0)/(u(i) - u0(i)) \end{aligned} \tag{4.17}$$

This is done for $i = 1, \ldots, p$ where p is the number of controls of the system.

4.2.3 Steady state error reduction method

The steady state error reduction method results a steady state error of zero between the linear and nonlinear models (under certain conditions). This method is often better than the Matlab or perturbation methods.

4.2.3a Linearization with respect to states

The nonlinear system represented by Equation 4.14 is run in closed loop until it reaches steady state. Then the steady state control inputs, states, and outputs are saved for later calculations (these are referred to as the nominal inputs, states, and outputs). Each state element is perturbed individually from their nominal values by some small percentage and then corresponding changes in the states, state derivatives, and outputs are observed at some small time greater than zero. The state, state derivative and output changes are saved as column vectors. After this procedure is repeated for each state element, the column vectors are augmented to form matrices. Then using the following equations, A and C matrices are computed.

$\Delta u = 0$; i.e., control inputs are not changed

$\Delta x_i = \text{change in } x \text{ vector due to change in } x_i$

$\Delta \dot{x}_i = \text{change in } \dot{x} \text{ vector (at some small nonzero time) due to change in } x_i$

$$\Delta x = [\Delta x_1 \quad \cdots \quad \Delta x_n]$$

$$\Delta \dot{x} = [\Delta \dot{x}_1 \quad \cdots \quad \Delta \dot{x}_n]$$

$$\begin{aligned} \Delta \dot{x}_1 &= A\Delta x_1 \\ &\vdots \\ \Delta \dot{x}_n &= A\Delta x_n \end{aligned}$$

$$[\Delta\dot{x}_1 \quad \cdots \quad \Delta\dot{x}_n] = A[\Delta x_1 \quad \cdots \quad \Delta x_n]$$

$$A = \Delta\dot{x}(\Delta x)^{-1} \tag{4.18}$$

Δy_i = change in y vector (at some small nonzero time) due to change in x_i

$$\Delta y = [\Delta y_1 \quad \cdots \quad \Delta y_n]$$

$$\Delta y_1 = C\Delta x_1$$
$$\vdots$$
$$\Delta y_n = C\Delta x_n$$

$$[\Delta y_1 \quad \cdots \quad \Delta y_n] = C[\Delta x_1 \quad \cdots \quad \Delta x_n]$$

$$C = \Delta y(\Delta x)^{-1} \tag{4.19}$$

where n is the number of states in the system

4.2.3b Linearization with respect to controls

Initially the system is linearized with respect to the states to find the system's A and C matrices (this linearization can be done using any available linearization method). Next perturbing the nominal control and running the system in open loop, find the steady state perturbation from the nominal state and output. The steady state error reduction method computes the B and D matrices that will force a zero difference between the nonlinear and linearized state and output perturbations.

Δu_i = change in control (u) vector after perturbing i^{th} element of u

Δx_i = steady state change in x vector after perturbing i^{th} element of u

$$0 = A\Delta x_1 + B\Delta u_1$$
$$\vdots \quad \vdots \quad \vdots$$
$$0 = A\Delta x_p + B\Delta u_p$$

$$0 = A[\Delta x_1 \quad \cdots \quad \Delta x_p] + B[\Delta u_1 \quad \cdots \quad \Delta u_p]$$

$$0 = A\Delta x + B\Delta u$$

$$B = -A\Delta x(\Delta u)^{-1} \tag{4.20}$$

Similarly, using the output perturbation, the D matrix is calculated as follows

Δy_i = steady state change in y vector after perturbing i^{th} element of u

$$[\Delta y_1 \quad \cdots \quad \Delta y_p] = C[\Delta x_1 \quad \cdots \quad \Delta x_p] + D[\Delta u_1 \quad \cdots \quad \Delta u_p]$$

$$\Delta y = C\Delta x + D\Delta u$$

$$D = (\Delta y - C\Delta x)(\Delta u)^{-1} \tag{4.21}$$

where p is the number of control inputs to the system.

4.3 Linearization of the MAPSS turbofan engine model

A turbofan engine is a highly nonlinear model. The turbofan model has to be linearized to estimate its health parameters by using the linearized Kalman filter technique described in Section 4.1.1. As described in the Section 4.2, there are three different types of linearization techniques that can be used to linearize the MAPSS model. The MAPSS model has to be linearized with respect to states, control inputs and health parameters. The type of linearization to be performed is specified by three different variables defined in the source code as *StateLin*, *ControlLin*, and *HealthLin*. Each of these three parameters can use one of the three linearization methods discussed in the previous section to linearize the turbofan model. This results in 27 different linearization combinations for a single MAPSS model. All of the 27 linear models are compared with the nonlinear MAPSS model and the results are discussed in Chapter VI.

4.4 Discretization of the MAPSS linear model

The linear approximation of the nonlinear MAPSS model obtained by one of the combinations discussed in Section 4.3 is represented by

$$\Delta\dot{x} = A\Delta x + B_u\Delta u + B_p\Delta p$$

$$\Delta y = C\Delta x + D_u\Delta u + D_p\Delta p \qquad (4.22)$$

where x is the state vector, u is the control input vector, p is the health parameter vector, and y is the sensor output vector (measurements) and

Equation 4.22 represents a continuous time system, but for the simplicity and to avoid complexity, the discretized model of this system is considered for the estimation of health parameters. The rate at which the system has to sampled or discretized is given by sampling time (T). The discretized system is represented by the following equations.

$$\Delta x_{k+1} = A'\Delta x_k + B'_u\Delta u_k + B'_p\Delta p_k$$

$$\Delta y_k = C'\Delta x_k + D'_u\Delta u_k + D'_p\Delta p_k \qquad (4.23)$$

where $A' \equiv e^{AT}$, $B'_u \equiv A^{-1}(e^{AT} - I)B_u$, $B'_p \equiv A^{-1}(e^{AT} - I)B_p$, $C' \equiv C$, $D'_u \equiv D_u$ and $D'_p \equiv D_p$ [20].

Since any Kalman filtering technique estimates only the states of the system, the other system parameters of interest that are to be estimated have to be augmented with the system states. This new augmented system will have different system matrices and

state vectors when considered with the original system. i.e., the new augmented system can be represented by

$$\Delta X_{k+1} = A_{aug}\Delta X_k + B_{aug}\Delta u_k$$

$$\Delta y_k = C_{aug}\Delta X_k + D'_u\Delta u_k \qquad (4.24)$$

where X is the augmented state vector, $A_{aug} = \begin{bmatrix} A' & B'_p \\ 0 & I \end{bmatrix}$; $C_{aug} = \begin{bmatrix} C' & D'_p \end{bmatrix}$;

$B_{aug} = \begin{bmatrix} B'_u \\ 0 \end{bmatrix}$ and $\Delta X = \begin{bmatrix} \Delta x \\ \Delta p \end{bmatrix}$

the size of *I* and 0 matrices depend on the sizes of state vector *x,* control input vector *u,* and health parameter vector *p.*

As discussed in Section 2.5, MAPSS model has 3 states, 3 control inputs, 11 sensor outputs and 10 health parameters to be estimated. Considering the above dimensions, the MAPSS system matrices will have the following dimensions.

A_{aug} **=13** × **13** ; (10 health parameters are augmented to 3 states)

B_{aug} **= 13** × **3** ; (3 control inputs)

C_{aug} **= 11** × **13** ; (11 sensor outputs)

D'_u **= 11** × **3**

Δx **= 3** × **1**

Δp **= 10** × **1**

Δu **= 3** × **1**

ΔX = **13** × **1** ; (augmented state vector)

The linearized Kalman filter technique is implemented on this augmented system to estimate the augmented state vector ΔX .

4.5 Discrete Linearized Kalman filter

The linearized Kalman filter discussed in Section 4.1.1 was for continuous time systems. However, for simplicity and reducing the complexity, the discrete model of the turbofan model is used in this research. The discretized form of the linearized Kalman filter uses the same five equations as discussed in Section 3.3 in the previous chapter except for the system matrices (*A, B, C* and *D*) are obtained by linearizing the nonlinear turbofan model at the nominal values. There are different equivalent Kalman filter equations that can be implemented in a more simple way compared to the conventional Kalman filter.

The type of linearized Kalman filter implemented in this research is the *a priori Kalman filter*. The typical five equations are reduced to three equations in this *a priori* filter. An *a priori* filter is one in which states and estimation error covariances are updated using their *a priori* values i.e., $\hat{x}_k^-$ and P_k^- .

Considering Equation 4.26 in Section 3.3 for *a priori* estimation error covariance we see that

$P_k^- = A_{k-1} P_{k-1}^+ A_{k-1}^T + Q'_{k-1}$ where $Q'_{k-1} \equiv \Lambda_{k-1} Q_{k-1} \Lambda_{k-1}^T$

The Kalman gain from Section 3.3 (Equation 4.27) is

$$K_k = P_k^- C_k^T [C_k P_k^- C_k^T + R_k]^{-1}$$

then by substituting the value of *a posteriori* value for estimation error covariance P_{k-1}^+ from Section 3.3 (Equation 4.29), the following equation is obtained.

$$P_k^- = A_{k-1} P_{k-1}^- A_{k-1}^T - A_{k-1} K_{k-1} C_{k-1} P_{k-1}^- A_{k-1}^T + Q'_{k-1}$$

From $K'_{k-1} \equiv A_{k-1} K_{k-1}$ we obtain

$$K'_{k-1} = A_{k-1} P_{k-1}^- C_{k-1}^T [C_{k-1} P_{k-1}^- C_{k-1}^T + R_{k-1}]^{-1} \quad (4.25)$$

The *a priori* value of estimation error covariance is

$$P_k^- = A_{k-1} P_{k-1}^- A_{k-1}^T - K'_{k-1} C_{k-1} P_{k-1}^- A_{k-1}^T + Q'_{k-1} \quad (4.26)$$

Now considering the state estimate update equations from Section 3.3, i.e., (Equation 4.25) we obtain

$$\hat{x}_k^- = A_{k-1} \hat{x}_{k-1}^+ + B_{k-1} u_{k-1}$$

Substituting the *a posteriori* estimate $\hat{x}_{k-1}^+$ from Equation 4.28 gives

$$\hat{x}_k^- = A_{k-1} \hat{x}_{k-1}^- + B_{k-1} u_{k-1} + K'_{k-1} (z_{k-1} - C_{k-1} \hat{x}_{k-1}^-) \quad (4.27)$$

Equations 4.25, 4.26 and 4.27 represent the *a priori* Kalman filter which are implemented in this research. The state estimate and estimation error covariance are updated using these three equations. The above derivations are discussed in more detail in [21].

4.6 Health estimation GUI

A graphical user interface is developed for the health estimation of a turbofan engine. This GUI is developed using Matlab's GUIDE software. Like any other GUI, the main aim of this health estimation GUI is to make the estimation process more user friendly. Figure 4.1 displays the health estimation GUI of a turbofan engine. The user can specify the estimation specifications like the type of estimation technique to be used, the type of constraint to be implemented and also the type of filter, like steady state or time varying. The linearization technique to be implemented can be specified using the linear model push button. Initial conditions like initial estimation error covariance and process noise covariance can also be specified.

The measurements that are to be used to estimate the health parameters can be selected from the sensor outputs. The user can select sensor outputs of interest or the default sensor set that is used in this research. Once the estimation is done, the estimation errors are displayed in the text box at the bottom along with the estimation technique.

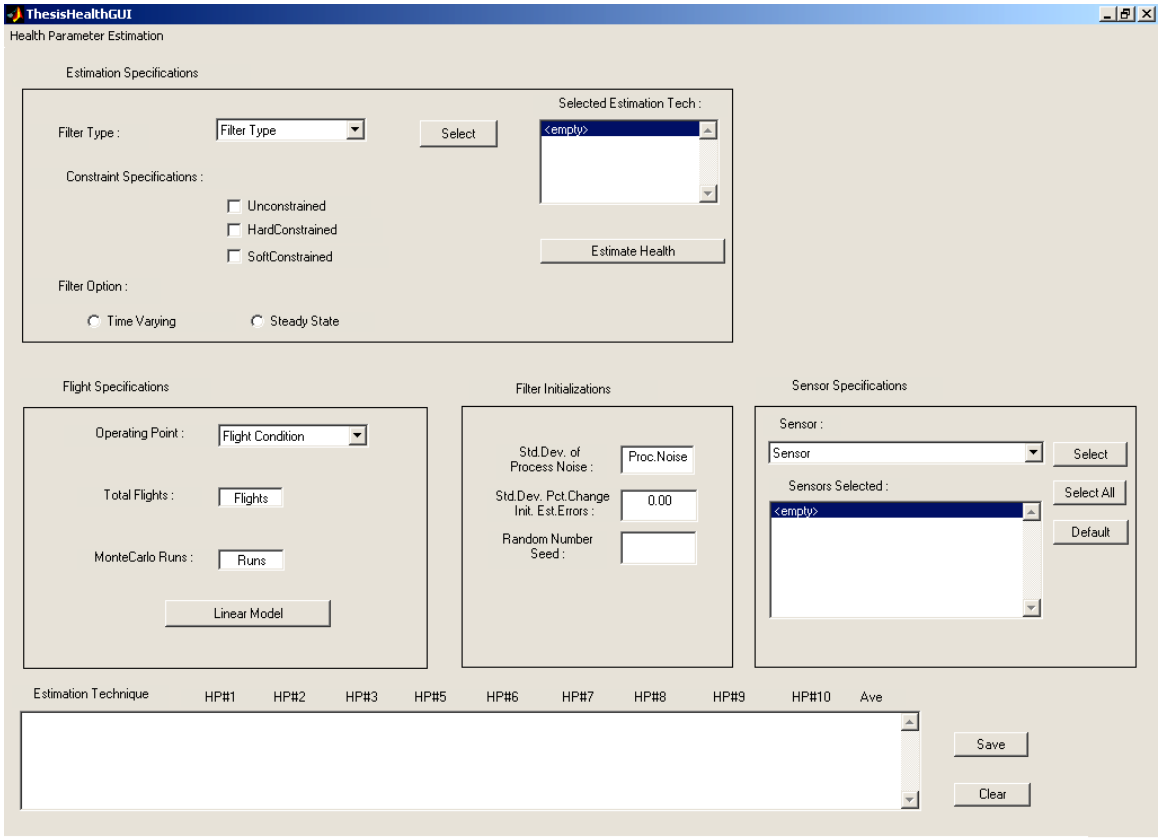

Figure 4.1: Health estimation GUI

CHAPTER V

SIMULATION RESULTS

The turbofan engine model is a highly nonlinear model. The model can be linearized so that the nonlinear estimation techniques can be implemented to estimate the model's health parameters. As discussed in Chapter IV, there are three different types of linearization techniques that can be used to linearize the MAPSS model. The type of linearization to be performed is specified by three different variables defined in the code as *StateLin*, *ControlLin*, and *HealthLin*. The linear models obtained are validated by comparing the trend of certain variables in the linear models with those in the nonlinear models over a period of time. Section 5.1 discusses the filtering results obtained from different linear models and their validation. The linearized Kalman filter was implemented on the MAPSS model to estimate the health parameters using all of the possible linear models. Both the unconstrained and constrained forms of the linearized Kalman filter estimates of the health parameters are shown in Section 5.2.

5. 1 Linearization of the MAPSS turbofan engine model

The MAPSS model was linearized with respect to states, control inputs and health parameters and each of these variables could be linearized in one of the three linearization techniques as discussed. This resulted in 27 different combinations of linearization techniques that can be applied to a single nonlinear MAPSS model.

The linearization method that is used is specified by the parameters *StateLin*, *ControlLin*, and *HealthLin* in the mapss_gui.m file. Each of these three parameters can be linearized in one of the three ways that we discussed previously.

States	0. Perturbation method
	1. Matlab method
	2. Steady state error reduction method
Controls	0. Perturbation method
	1. Matlab method
	2. Steady state error reduction method
Health Parameters	0. Perturbation method
	1. Matlab method
	2. Steady state error reduction method

Three values have been assigned to each of these parameters (*StateLin*, *ControlLin*, and *HealthLin*) to describe how they would be linearized. For instance, the **Perturbation Method** is specified with a parameter value of **0**, the **Matlab method** is specified with a parameter value of **1**, and the **Steady state error reduction method** is specified with a parameter value of **2**.

Validation

All 27 models were compared with the nonlinear model. The linear model that resulted in minimum errors or deviations of the 22 sensor outputs from the nonlinear model is the best linearized model of all the 27 combinations. This linearization test is performed by perturbing the health parameters and initial states by some percentage of their initial values. If there was no perturbation then both the linear and nonlinear model would behave identically.

Each linearization technique can be used with a different perturbation value. We used three different linearization perturbation values (0.01%, 0.1% and 0.5% of the steady state value). We then tested the linear models that resulted with three different test perturbation values (0.01%, 0.1% and 0.5%). There are two types of errors that we considered for the validation of the linearization.

a) RMS Average Error

b) RMS Final Error

RMS average error is the average of the error over the whole time of the simulation (six seconds), and the RMS Final error is the error at the final time of simulation (i.e., at time = six seconds). The following tables show the best linearization method for each combination of linearization perturbation and test perturbation.

In Tables I and II, LIN*xyz* represents one of 27 linearization combinations.

x = *StateLin* (0, 1, or 2)

y = *ControlLin* (0, 1, or 2)

z = *HealthLin* (0, 1, or 2)

TABLE I – Best RMS errors averaged over the entire simulation time. LINxyz means state linearization x, control linearization y, health parameter linearization z. 0 means perturbation linearization, 1 means Matlab linearization, 2 means steady state error reduction method.

	Testing Perturbation Value (%)			
		0.01	**0.1**	**0.5**
Linearization Perturbation Value (%)	**0.01**	LIN212	LIN212	LIN212
	0.1	LIN212	LIN212	LIN212
	0.5	LIN212	LIN212	LIN212

Table I shows that the use of the steady state error reduction method for state linearization and health parameter linearization, combined with the Matlab linearization method for control input linearization, results in the best match between the linear and nonlinear models (when average RMS difference is considered).

TABLE II – Best RMS errors at the final time. LINxyz means state linearization x, control linearization y, health parameter linearization z. 0 means perturbation linearization, 1 means Matlab linearization, 2 means steady state error reduction method.

	Testing Perturbation Value (%)			
		0.01	**0.1**	**0.5**
Linearization Perturbation Value (%)	**0.01**	LIN022	LIN022	LIN122 LIN022
	0.1	LIN022	LIN022	LIN022
	0.5	LIN022	LIN022	LIN022

Table II shows that the use of the perturbation method for state linearization, and the steady state error reduction method for control and health parameter linearization, results in the best match between the linear and nonlinear models (when final RMS difference is considered).

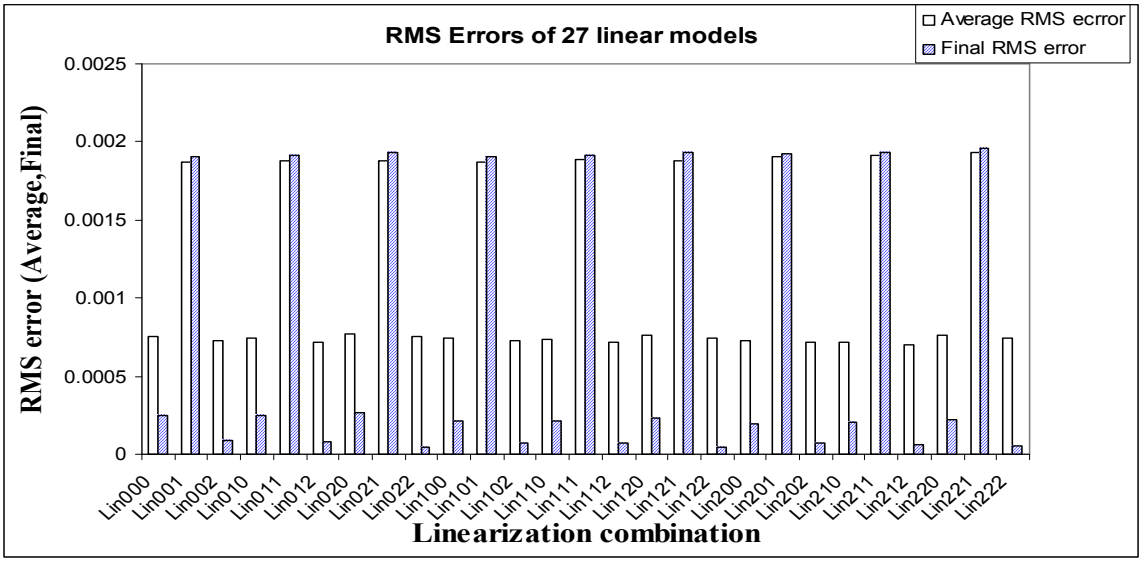

Figure 5.1: RMS errors of 27 linear models

The linearization techniques can be grouped into two categories based on the value of RMS errors as shown in Figure 5.1. All the linearization techniques in which the model is linearized with respect to health parameters in the Matlab method resulted in the worst RMS errors (LINxy1). All the other linearization techniques except the above case give similar results. It can also be observed that error bars exhibit a sequential pattern for all linearization techniques with a range of medium, high and low errors consecutively for sequential three linear combinations (bars in Figure 5.1).

Figure 5.2 shows the behavior of four different parameters of the linearized model (LIN002) with their corresponding nonlinear behavior. The solid lines represent the nonlinear behavior and dashed lines represent the linear behavior of the same parameter. Ground term in the label means that the engine is operated at the 1st operating point (PLA = 21, mach number = 0, altitude = 0) and *dpPct* specifies the percentage of perturbation in the health parameters by which the model is linearized. As seen there is not much variation in the trend of the parameters in the linear and nonlinear case.

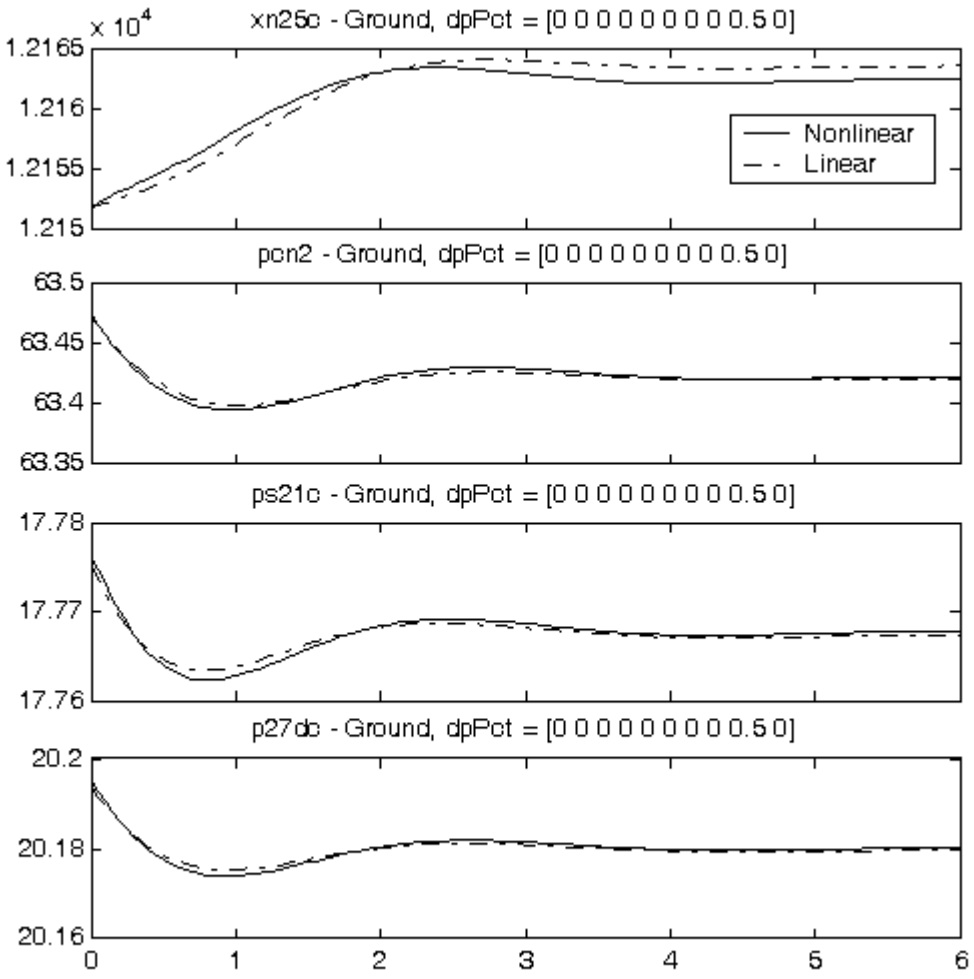

Figure 5.2: Linear Vs Nonlinear simulations

The average and final RMS error between the linear and nonlinear models for 27 different linearization combinations is shown in Table III. This table represents the RMS errors with perturbation values of 0.01% for linearization, and perturbation values of 0.01% for testing the linear models. The best performances are in boldface font.

TABLE III – Linear models performance. LINxyz means state linearization x, control linearization y, health parameter linearization z. 0 means perturbation linearization, 1 means Matlab linearization, 2 means steady state error reduction method.

Linearization Combination	***Average RMS Error □ 10^{-4}***	***Final RMS Error □ 10^{-4}***
Lin000	7.52	2.45
Lin001	18.72	19.05
Lin002	7.29	0.85
Lin010	7.45	2.49
Lin011	18.83	19.17
Lin012	7.20	0.81
Lin020	7.74	2.62
Lin021	18.75	19.31
Lin022	7.49	**0.42**
Lin100	7.44	2.12
Lin101	18.74	19.02
Lin102	7.26	0.73
Lin110	7.38	2.16
Lin111	18.85	19.14
Lin112	7.18	0.68
Lin120	7.61	2.27
Lin121	18.79	19.34
Lin122	7.42	0.43
Lin200	7.26	1.96
Lin201	19.09	19.23
Lin202	7.14	0.72
Lin210	7.16	2.03
Lin211	19.19	19.35
Lin212	**7.01**	0.65
Lin220	7.65	2.21
Lin221	19.31	19.55
Lin222	7.48	0.53

It can be seen that several of the linearization combinations provide performance nearly as good as the best linearization, but some linearization combinations perform quite poorly. The linearization technique in which the nonlinear model is linearized with respect to health parameters in perturbation method or steady state error reduction method was giving the best RMS errors. From the above results, it can be concluded that linear models obtained with the perturbation method or steady state error reduction would behave more close to the nonlinear systems than those obtained with the Matlab method.

5. 2 Health parameter estimation

The turbofan engine's health parameters are estimated based on some linear model. The linearized Kalman filter was implemented to estimate all 10 health parameters of the MAPSS model of the turbofan engine. However, due to an error in the MAPSS software health parameter # 4 cannot be estimated (i.e., it is completely unobservable, with no connection to the states or outputs). Two different algorithms were tested for estimating the health parameters: constrained Kalman filtering and unconstrained (standard) Kalman filtering.

As discussed in Section 4.4, the discrete linear model of the MAPSS model is obtained and is then augmented with the health parameters. The Kalman filter works on the principle of utilizing the known dynamics of the system (model) along with the measurements obtained from the model to estimate the states. Three seconds of data are collected at 10 Hz every flight. The model is simulated for 6 seconds so the states reach the steady state. The necessary measurements were obtained offline using the nonlinear model. The

model is linearized every 100 flights but the measurements were obtained every flight (for 3 sec) from the measurement files.

The list of health parameters that are to be estimated are given as follows.

1) Fan airflow
2) Fan efficiency
3) Booster tip airflow
4) Booster tip efficiency (unobservable in MAPSS)
5) Booster hub airflow
6) Booster hub efficiency
7) High pressure turbine airflow
8) High pressure turbine efficiency
9) Low pressure turbine airflow
10) Low pressure turbine efficiency

The sensor measurements used to estimate the above health parameters are given as follows with their corresponding SNR (signal-to-noise ratios) values as shown. These signal-to-noise ratios were determined on the basis of NASA experience and previously published data [28].

1) LPT exit pressure (SNR = 100)
2) LPT exit temperature (SNR =100)
3) Percent low pressure spool rotor speed (SNR =150)
4) HPC inlet temperature (SNR =100)

5) HPC exit temperature (SNR =200)

6) Bypass duct pressure (SNR =100)

7) Fan exit pressure (SNR =200)

8) Booster inlet pressure (SNR =200)

9) HPC exit pressure (SNR =100)

10) Core rotor speed (SNR =150)

11) LPT blade temperature (SNR =70)

The health parameter degradation estimation is performed at two different engine operating conditions. These operating conditions represent the conditions where the engines actually operate for a long period of time.

5.2.1 Unconstrained Kalman filter estimates

The results were obtained based on a Monte Carlo simulation of 20 experiments. As discussed in Section 4.4, the state vector of the dynamic MAPSS model is augmented to include the health parameters, which are then estimated with a linearized Kalman filter. Initially the standard Kalman filter (unconstrained) is implemented on the turbofan model and the change in health parameters is estimated. The time varying form of the standard Kalman filter is implemented in this thesis instead of a steady state filter to get more accurate results. Table IV shows the RMS estimation errors over 50 flights of the unconstrained Kalman filter for each of the health parameters of all 27 possible linearized models (health parameter # 4 is not included for the reasons discussed above). The linearization combinations displayed are similar to the linear models described in the Section 5.1.

TABLE IV – RMS health parameter (degradation) estimation errors (percent) for the unconstrained Kalman filter for 27 linear models. LINxyz means state linearization x, control linearization y, health parameter linearization z. 0 means perturbation linearization, 1 means Matlab linearization, 2 means steady state error reduction method

Linearization	***Health Parameter***									
Combination	***1***	***2***	***3***	***5***	***6***	***7***	***8***	***9***	***10***	***Average***
000	18.41	2.18	16	6.84	2.54	2.43	6.16	3.19	8.71	7.38
001	18.69	2.14	15.71	5.13	7.95	2.29	7.1	2.65	8.78	7.83
002	17.62	2.33	16.56	7.36	2.22	3.29	6.9	3.99	9.22	7.72
010	18.54	2.48	16.02	7.04	2.25	2.77	6.72	3.13	8.81	7.53
011	17.4	2	15.51	5.31	7.77	2.58	7.4	**2.57**	8.79	7.7
012	16.38	2.58	16.2	7.64	2.61	3.34	6.29	3.86	9.01	7.54
020	18.26	2.08	16.08	4.75	2.7	2.48	6.66	3.49	9	7.28
021	18.05	2.36	**15.14**	**2.92**	7.91	2.69	7.14	3.36	9.08	7.63
022	17.94	2.43	15.52	5.45	2.16	3.79	6.48	4.31	9.23	7.48
100	**16.16**	2.46	16.32	7.08	2.59	2.77	**5.79**	2.96	**8.52**	7.18
101	17.77	2.15	15.55	4.78	7.58	2.64	7.14	2.91	8.86	7.71
102	16.49	2.34	16.29	7.64	2.31	2.84	6.01	3.84	8.93	7.41
110	17.04	2.39	16.17	6.74	2.26	2.65	5.86	3.21	8.64	7.22
111	18.37	2.03	15.43	5.22	7.65	2.76	7.15	2.59	8.75	7.77
112	19.05	**1.97**	16.19	7.54	2.73	3.11	6.19	4.01	9.03	7.76
120	17.02	2.36	15.44	4.27	2.31	2.85	6.5	3.64	9.02	**7.04**
121	16.88	2.26	15.76	3.37	8.05	2.8	7.19	2.99	8.94	7.57
122	18.25	2.2	16.4	5.5	2.22	3.54	6.77	4.61	9.42	7.66
200	17.15	2.52	15.59	6.14	2.31	**2.24**	6.29	3.146	8.71	7.12
201	18.92	2.23	15.57	4.65	7.69	2.64	7.23	2.82	8.8	7.84
202	16.27	2.64	16.13	6.93	2.3	3.64	6.39	3.62	8.94	7.43
210	17	2.11	15.89	5.77	2.35	2.6	6.25	3.11	8.68	7.08
211	19.57	2.26	15.48	4.82	7.9	2.61	7.03	2.62	8.73	7.89
212	17.86	2.42	16.26	6.35	2.26	3.26	6.98	3.49	9.07	7.55
220	18.79	2.25	15.36	4.67	2.25	2.53	6.64	3.65	9.02	7.24
221	18.44	2.22	15.24	3.99	7.91	2.54	7.24	3.12	9	7.75
222	18.21	2.23	15.85	5.47	**2.14**	3.67	6.72	4.41	9.33	7.56

A wide variety of Kalman filter performance is shown in Table IV, depending on which linearization combination is used. Overall, it appears that using the Matlab method for the state linearization, the steady state error reduction method for the control linearization, and the perturbation method for the health parameter linearization, results in the best Kalman filter performance.

Figure 5.3a is a graphical representation of the effect of the 27 linearization techniques on the unconstrained Kalman filter performance for the health estimation of the turbofan engine at operating point where PLA = 21, mach number = 0, altitude = 0. There is not much variation in the results; however it can be shown that the linear model where the health parameters were linearized in Matlab method resulted in bad estimation errors.

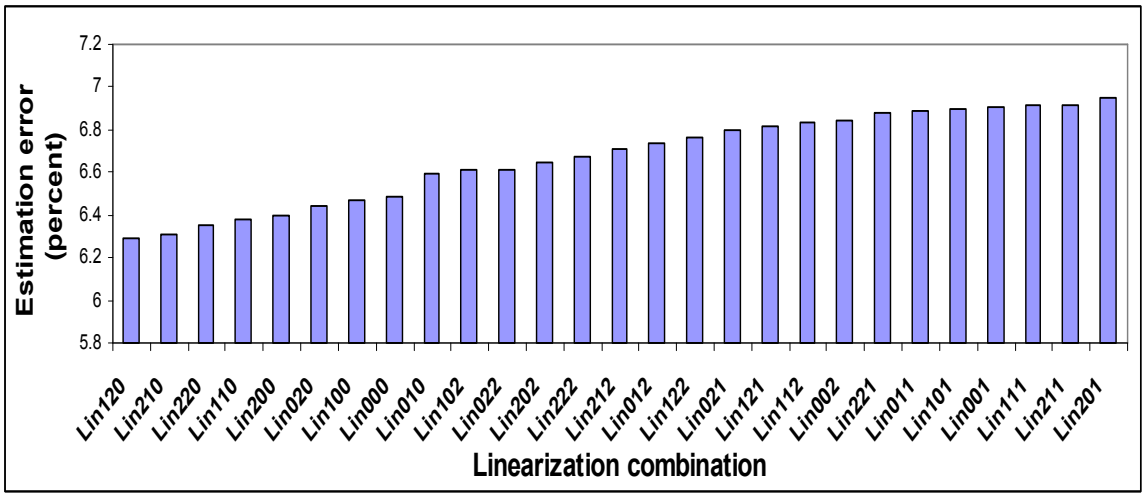

Figure 5.3a: Unconstrained RMS health parameters degradation estimation errors (percent) for 1st operating condition.

5.2.2 Constrained Kalman filter estimates

In the application of Kalman filters there is often known model or signal information that is either ignored or dealt with heuristically [29]. State variable constraints (which may be based on physical considerations) are often neglected because they do not fit easily into the structure of the Kalman filter. Using one of the two analytic methods of incorporating state variable inequality constraints in the Kalman filter as discussed in [29], the change in health parameters are estimated. This method of enforcing the state variable constraints in to the Kalman filter structure is performed using the hard constraints. Engine health always deteriorates over time, and this information can be incorporated into the Kalman filter structure as a state variable constraint. This incorporation of state variable constraints increases the computational effort of the filter but significantly improves its estimation accuracy [10]. The inequality state variable constraints are considered to be linear in this estimation problem from the fact that the health parameters can never improve, i.e., the change in the state variables can be zero or negative but cannot be positive from one time step to next. This constrained estimation problem of inequality constraints can be solved using a quadratic programming algorithm. The incorporation of inequality constraints and then solving them, results in a new filter which is a combination of standard Kalman filter and a quadratic programming problem.

Constrained estimation is performed by projecting the unconstrained estimate on to the constraint surface at each time step and then solving the inequality constraint problem using quadratic programming. A family of constrained state estimates is

obtained, where the weighting matrix of the quadratic programming problem determines which family member forms the desired solution [10].

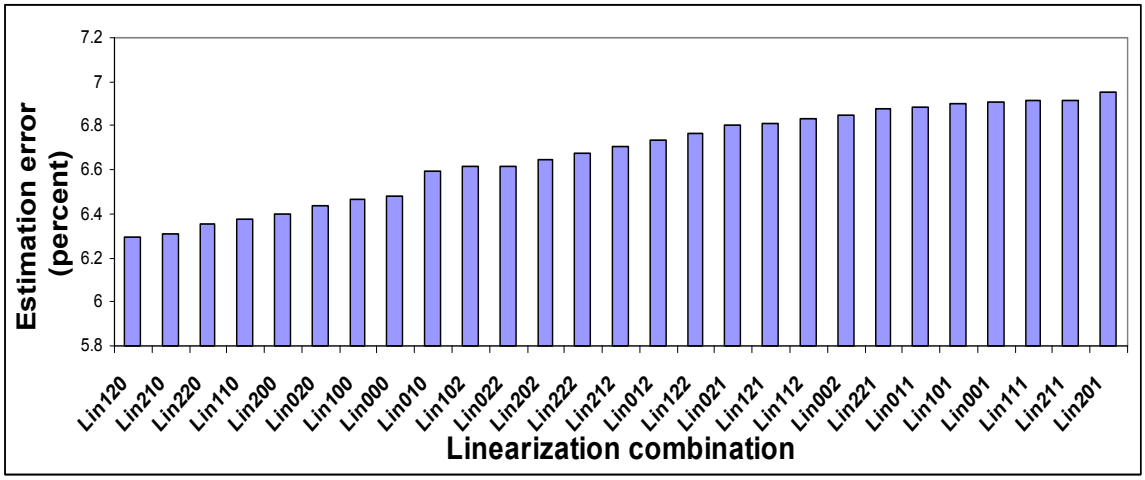

Figure 5.3b: Constrained RMS health parameters degradation estimation errors (percent) for 1st operating condition.

Similar to Figure 5.3a, the effect of 27 linearization combinations on the constrained Kalman filter performance is shown in Figure 5.3b. Though, it is shown that using the Matlab method for the state linearization, the steady state error reduction method for the control linearization, and the perturbation method for the health parameter linearization, resulted in the best Kalman filter performance, there are other linearization combinations that resulted in good estimates too. The Kalman filter implementation with the linearization method which is considered to be best by comparing linear and nonlinear simulations resulted in estimates that are close to the best estimates.

TABLE V – RMS health parameter (degradation) estimation errors (percent) for the constrained Kalman filter for 27 linear models. LINxyz means state linearization x, control linearization y, health parameter linearization z. 0 means perturbation linearization, 1 means Matlab linearization, 2 means steady state error reduction method

Linearization	***Health Parameters***									
Combination	***1***	***2***	***3***	***5***	***6***	***7***	***8***	***9***	***10***	***Average***
000	13.42	2.09	14.67	6.78	2.25	2.15	5.8	2.78	8.37	6.48
001	13.61	1.92	14.41	5.08	7.49	2.08	6.87	2.18	8.45	6.9
002	13.45	2.25	14.79	7.31	2.07	2.87	6.47	3.52	8.86	6.84
010	13.3	2.42	14.58	6.97	2.01	2.49	6.37	2.68	8.45	6.58
011	12.97	**1.82**	14.36	5.27	7.38	2.34	7.18	**2.15**	8.48	6.88
012	**12.6**	2.36	14.66	7.62	2.38	2.9	5.94	3.44	8.71	6.73
020	13.86	1.95	14.69	4.77	2.43	2.15	6.29	3.08	8.68	6.43
021	13.56	2.14	**14.13**	**2.89**	7.47	2.37	6.96	2.87	8.77	6.8
022	13.18	2.33	14.29	5.48	**1.94**	3.36	6.13	3.8	8.92	6.61
100	12.74	2.47	14.85	7.03	2.36	2.45	**5.46**	2.59	**8.21**	6.46
101	13.32	1.99	14.48	4.67	7.18	2.42	6.95	2.49	8.56	6.9
102	12.76	2.19	14.75	7.6	2.08	2.42	5.64	3.43	8.61	6.61
110	12.79	2.25	14.64	6.66	2.06	2.37	5.49	2.8	8.28	6.37
111	13.53	1.88	14.33	5.15	7.21	2.51	6.95	2.16	8.44	6.91
112	13.99	1.86	14.74	7.46	2.59	2.75	5.82	3.58	8.69	6.83
120	12.89	2.32	14.36	4.27	2.08	2.5	6.21	3.23	8.73	**6.29**
121	13.04	2.11	14.5	3.28	7.64	2.51	6.99	2.57	8.65	6.81
122	13.76	2.08	14.74	5.56	2.06	3.08	6.35	4.1	9.09	6.76
200	13.35	2.38	14.44	6.09	2.04	**1.98**	6.03	2.81	8.43	6.39
201	13.74	2.1	14.45	4.6	7.3	2.43	6.99	2.36	8.54	6.95
202	12.63	2.57	14.54	6.96	2.08	3.2	6	3.2	8.61	6.64
210	12.81	2.1	14.59	5.75	2.14	2.32	5.94	2.74	8.37	6.31
211	13.89	2.082	14.32	4.78	7.5	2.32	6.77	2.16	8.39	6.91
212	13.81	2.17	14.68	6.36	2.09	2.82	6.62	3.04	8.74	6.7
220	13.49	2.2	14.29	4.66	2	2.22	6.33	3.22	8.72	6.35
221	13.46	2.09	14.19	3.97	7.5	2.24	7.06	2.66	8.71	6.88
222	13.36	2.11	14.53	5.51	1.96	3.24	6.37	3.94	9	6.67

Table V shows the performance of the constrained Kalman filter, depending on which linearization combination is used. As with the standard Kalman filter, it appears that using the Matlab method for the state linearization, the steady state error reduction method for the control linearization, and the perturbation method for the health parameter linearization, results in the best constrained Kalman filter performance.

Figure 5.3a and 5.3b show that Kalman filter performance is quite bad when the model is linearized with respect to health parameters in Matlab method. This proves that Kalman filter performance mainly depends on the linearization accuracy of the nonlinear model. Hence, accurate estimates can only be obtained by implementing Kalman filter on the linear models that behave as close as possible to their nonlinear models.

When average health parameter degradation estimation error (percent) is considered in Tables IV and V, the constrained filter has a smaller estimation error than the unconstrained filter. This is because the constrained state estimate is unbiased and has a smaller error covariance than the unconstrained estimate. But this (extra accuracy) is achieved at the additional computational effort of performing quadratic programming algorithm at each time step.

Figure 5.4a and 5.4b show the health parameter degradation estimations of unconstrained filter and constrained filter with the true degradation for 500 flights respectively. The thick lines show the true degradation of the health parameters and thin lines represent their corresponding estimations. The true health parameters degradations

are plotted by certain exponential functions which are the approximations of the turbofan health parameters degradations. These approximations are based on NASA experience from the real time flight data. It can be seen from the Figures 5.2a and 5.2b, that there are only five thick lines corresponding to the nine thin lines, this is because the true degradation of certain health parameters are the same.

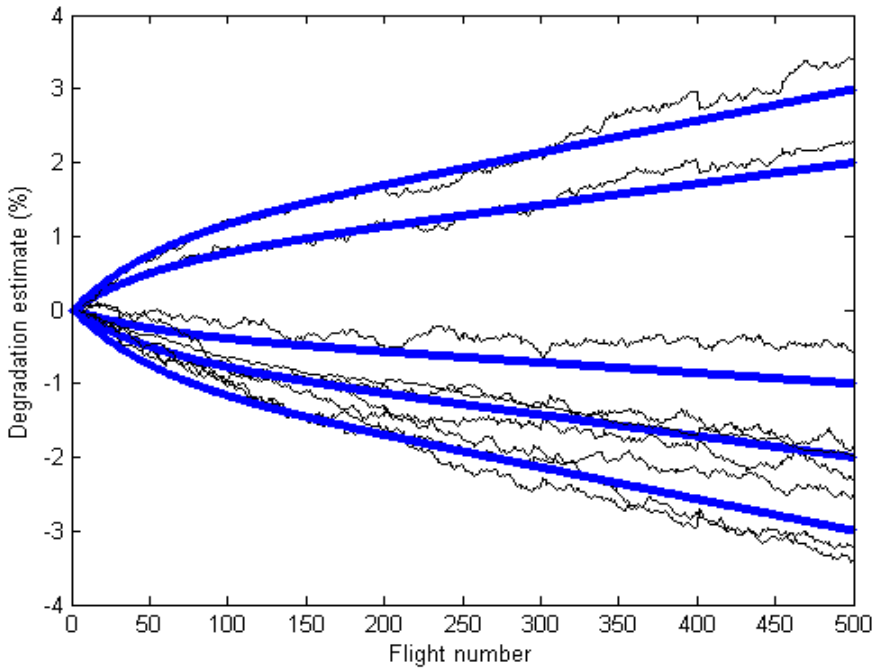

Figure 5.4a: Unconstrained health parameter degradation estimates

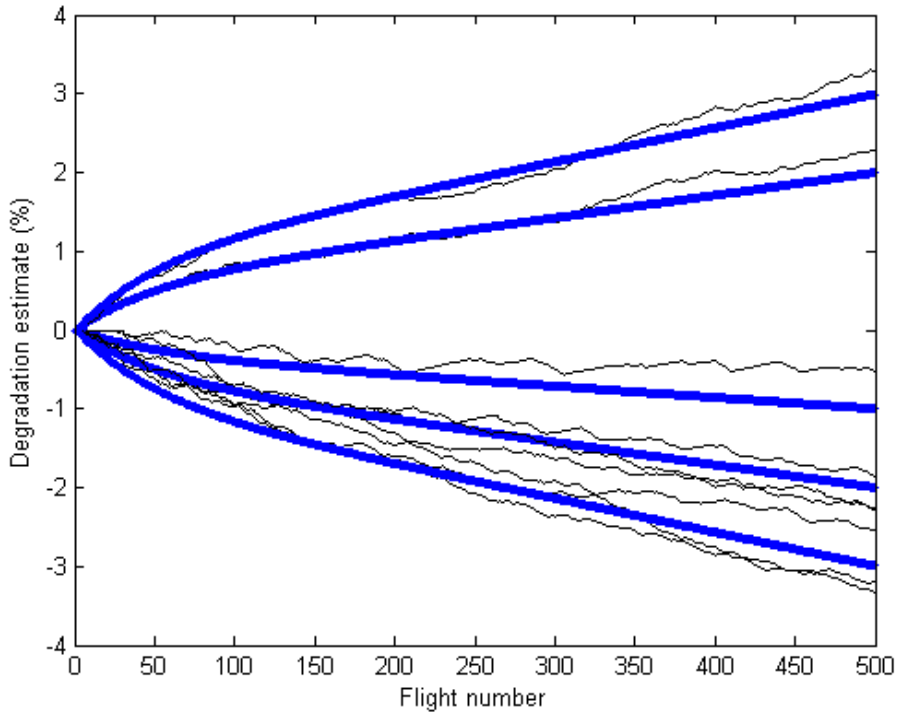

Figure 5.4b: Constrained health parameter degradation estimates

Figures 5.5a and 5.5b show the health parameters estimation errors of turbofan engine for 27 linear models with operating point of PLA = 35, Mach Number = 0.8 and altitude = 35000. The steep increase in the last 9 linear models is because of the model being linearized in Matlab method with respect to health parameters.

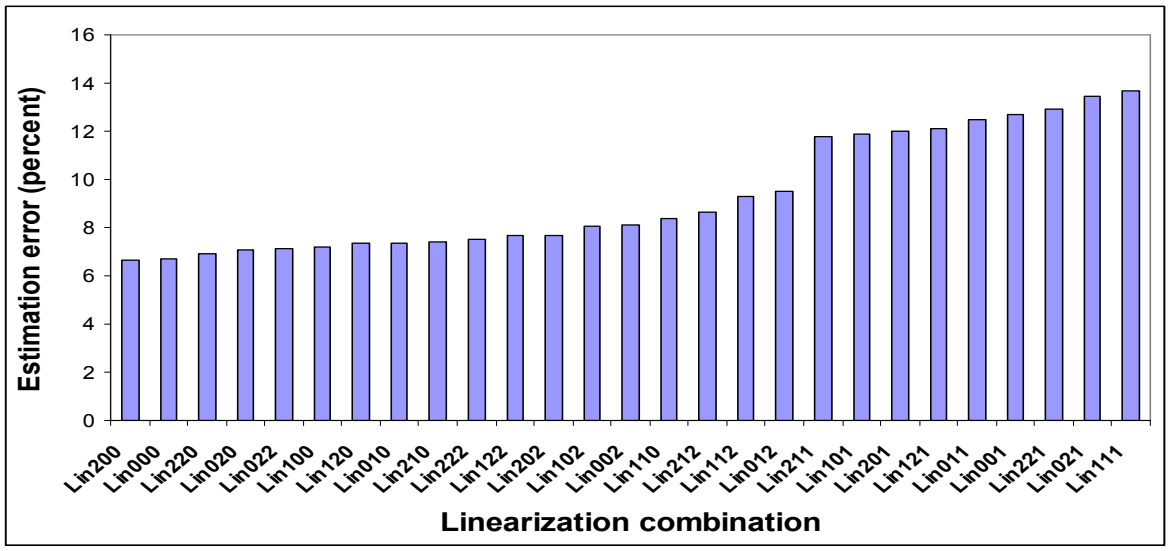

Figure 5.5a: Unconstrained RMS health parameters degradation estimation errors (percent) for 2nd operating condition

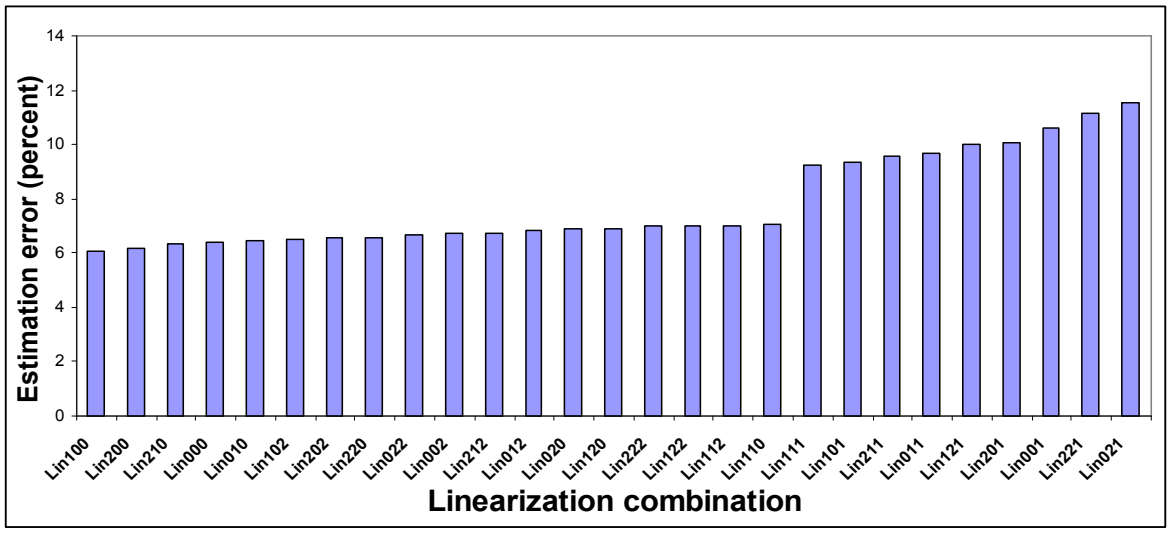

Figure 5.5b: Constrained RMS health parameters degradation estimation errors (percent) for 2nd operating condition

CHAPTER VI

UNSCENTED KALMAN FILTER

The extended Kalman filter is considered to be the most widely used recursive estimation algorithm for the nonlinear systems. In this chapter we discuss the major flaws and assumptions that are encountered in the EKF algorithm and discuss a new estimation algorithm to overcome those flaws. Years of research in the estimation field has resulted in many different algorithms which have their own pros and cons. The unscented Kalman filter is one of those algorithms. This UKF algorithm was first proposed by Julier et al. [22] and was further developed by Wan and van der Merwe [23]. This UKF is based on the unscented transformation of the mean and covariance of the parameters to be estimated.

Estimating the states of a nonlinear system is extremely difficult. The optimal solution to this estimation requires the propagation of the full PDF (probability density function) of the states through the time update. This propagation is almost impossible because the PDF of any variable is not finite (restricted). However, an approximation of

some kind is considered for this PDF in estimation algorithms. The Kalman filter uses the first two moments (mean and covariance) of the state distribution in its update rules. There are a couple of reasons to consider only mean and covariance. Firstly, the mean and covariance of the unknown distribution requires the maintenance of a small and constant amount of information. Secondly, both the mean and covariance are linearly transformable quantities. For example, if a distribution has the mean M and covariance C, after the linear transformation T, the mean and covariance will be TM and TCT'.

The EKF basically works on the assumptions that all the transformations are linear. The EKF is an estimation algorithm wherein the nonlinear system is linearized first and then the recursive Kalman filter equations are applied for the time update. Linearizing the nonlinear system involves the calculation of Jacobians and substituting them for the linear transformation in the KF equations. The EKF is difficult to tune and may result in unreliable estimates if the nonlinearities are severe. The major limitations of the EKF are

1) The EKF can be applied only if the Jacobians can be calculated.

2) Jacobian calculation is an extremely difficult and error-prone process.

3) Linearization is based on the Taylor series approximation, considering only the first two terms of the series and ignoring the other higher order terms.

As the EKF totally depends on the linearization to propagate the mean and covariance, it is obvious that EKF would give bad estimates if any one of the above limitations is encountered.

To overcome these limitations, the unscented transformation was derived which utilizes a more direct and simple approach to propagate the mean and covariance. The main advantage of implementing unscented transformation on a nonlinear estimation problem is that it approximates the mean to third order, which is better than linearization, and it approximates the covariance to third order, which is the same as linearization. Section 6.1 discusses the basic unscented transformation on which UKF was derived. The UKF algorithm will be derived in Section 6.2. Section 6.3 describes reduced sigma point filters and finally the performance of the UKF is shown by an inverted pendulum application in Section 6.4 and its corresponding simulation results in Section 6.5.

6.1 Unscented Transformation

The unscented transformation is a method for calculating the statistics of a random variable which undergoes a nonlinear transformation [7]. The unscented transformation is based on two fundamental principles. First, it is easy to perform a nonlinear transformation on a single point (rather than an entire PDF). Second, it is not too hard to find a set of points in state space whose probability density function (PDF) approximates the true PDF of a state vector [24].

Consider a random variable ***x*** with dimension ***n*** which is going through a nonlinear transformation, *y=f(x).* Initial condition states that *x* has a mean $\bar{x}$ and covariance P_x. The unscented transformation calculates the statistics of *y* by forming a set of sigma points (vectors) X_i. These sigma points should be chosen such that they capture the most important statistical properties of the prior random variable *x*. Sigma points are calculated according to the following conditions:

$$X_0 = \bar{x},$$

$$X_i = \bar{x} + (\sqrt{(L+\lambda)P_x})_i \quad i=1,\ldots\ldots L,$$

$$X_i = \bar{x} - (\sqrt{(L+\lambda)P_x})_i \quad i=L+1,\ldots\ldots,2L, \tag{6.1}$$

where $\lambda = \alpha^2(L+\kappa) - L$, is a scaling parameter. The constant α determines the spread of the sigma points around $\bar{x}$ which is usually set to a small positive value ($0<\alpha<1$). κ is a secondary scaling parameter which is set to *3–L*. (set to 0 in our case). $(\sqrt{(L+\lambda)P_x})_i$ is the *i*th column of the matrix square root. This matrix square root can be obtained by using the Cholesky factorization routine in Matlab.

Each of the sigma vectors is assigned with a weight. These weights are calculated by the following equations.

$$W_0^{(m)} = \lambda/(L+\lambda)$$
$$W_0^{(c)} = W_0^{(m)} + 1 - \alpha^2 + \beta$$

$$W_i^{(c)} = W_i^{(m)} = 1/2(L+\lambda) \qquad i=1,\ldots\ldots 2L \tag{6.2}$$

where β is a factor that incorporates a prior knowledge of the distribution, usually set to 2 (set to $1-\alpha^2$ in our case).

The sigma vectors described in Equation 6.1 are propagated through the nonlinear function *y=f(x)* individually and the corresponding Y_i are obtained as

$$Y_i = f(X_i) \qquad i=0,\ldots\ldots,\ 2L, \tag{6.3}$$

The mean and covariance of the *y* are approximated using the above nonlinearly transformed sigma points (Y_i) and the weights by the following equations.

$$\bar{y} = \sum_{i=0}^{2L} W_i^{(m)} Y_i \tag{6.4}$$

$$P_y = \sum_{i=0}^{2L} W_i^{(c)} (Y_i - \bar{y})(Y_i - \bar{y})^T \tag{6.5}$$

Hence, $\bar{y}$ and P_y obtained in Equations 6.4 and 6.5 are the approximated mean and covariance of the nonlinearly transformed *x*. Figure 6.1 shows how the sigma points are nonlinearly transformed [22].

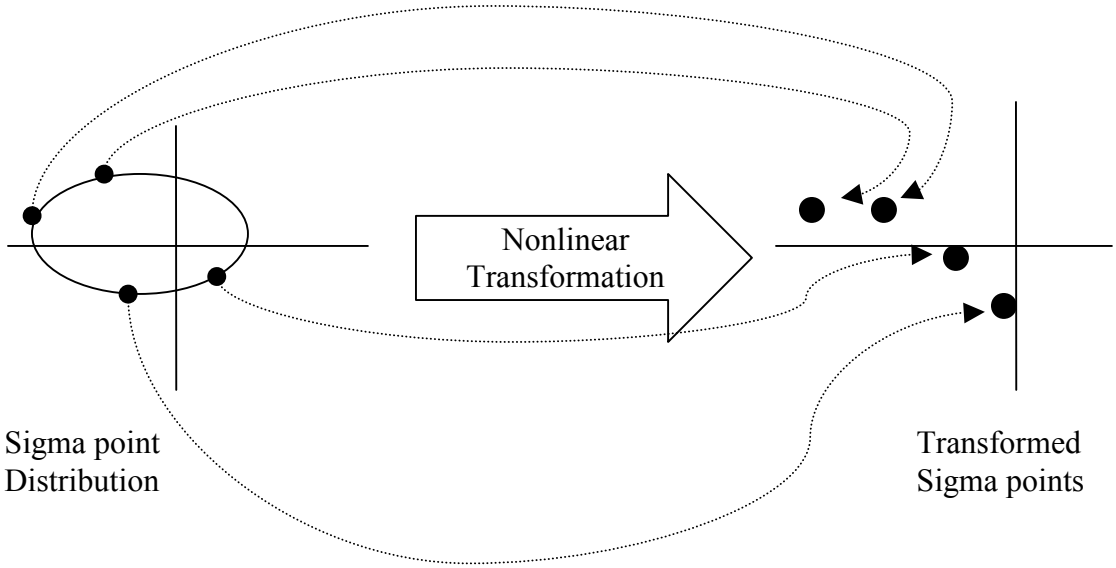

Figure 6.1: Principle of Unscented Transformation

6.2 Unscented Kalman filter

Estimating the states of the system is performed by propagating the mean and covariance of the state distribution. For linear systems, the general recursive Kalman filter algorithm based on MMSE (minimum mean squared error) is the straightforward estimation technique to be implemented. On the other hand, for nonlinear systems, the hybrid extended Kalman filter (EKF) is considered to be the best nonlinear estimator. However, as discussed previously, the EKF has some limitations as it is based on the linearization of the nonlinear system and also on some other approximations. The unscented Kalman filter is an alternative to the EKF which has the implementation of unscented transformation of the nonlinear state distribution and then applying the

recursive Kalman filter algorithm for the time update and measurement update for the nonlinearly transformed state distribution.

The unscented transformation is proved to be more accurate in propagating the mean and covariance when compared with the linearization method used in EKF.

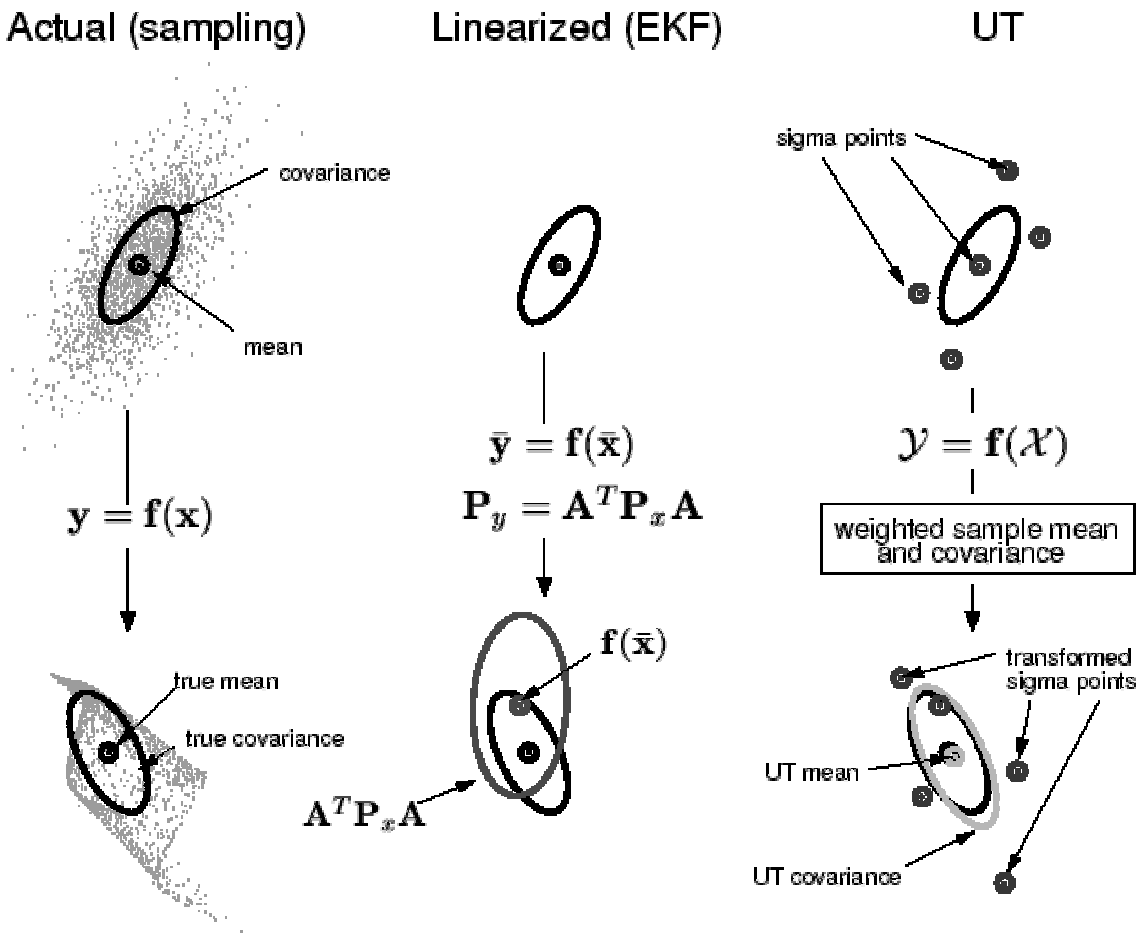

Figure 6.2: Mean and Covariance propagation in (a) Actual nonlinear transformation, (b) Extended Kalman filter (first order linearization), (c) Unscented Transformation

Figure 6.2 illustrates the mean and covariance propagation in all three transformations [23]. The mean in the EKF and UT are similar to that of the true nonlinear transformation. But, when covariance propagation is considered, the UT outperforms the EKF. And moreover there is no need of calculating any Jacobians in the unscented transformation algorithm. The order of computational effort is almost the same in both algorithms. When the computational effort is same in both cases, the unscented transformation is preferred over the EKF for the better accuracy.

The unscented Kalman filter algorithm can be divided in to three sections. The first part is the initialization of the state estimate and state covariance of the nonlinear system. The second part is applying the UT to the state distribution and calculating the a priori state estimate and a priori state covariance. The third part is performing the measurement update equations and calculating the Kalman gain, state estimate and state error covariance.

6.2.1 Algorithm for additive noise (zero mean)

Consider a discrete time nonlinear system represented by

$$\begin{aligned} x_{k+1} &= f(x_k, u_k, t_k) + w_k \\ y_k &= h(x_k, t_k) + v_k \end{aligned} \tag{6.6}$$

where $w_k \sim N(0, Q_k)$, $v_k \sim N(0, R_k)$ are additive process and measurement noise, with zero mean and covariances of Q_k and R_k .

Initialization

The UKF is initialized with the initial estimate and estimation error covariance as in the EKF.

$$\hat{x}_0^+ = E(x_0)$$
$$P_0^+ = E[(x_0 - \hat{x}_0^+)(x_0 - \hat{x}_0^+)^T] \tag{6.7}$$

Sigma point selection

As seen previously in the unscented transformation, a set of sigma points and their corresponding weights are calculated around the initial estimate according to Equation 6.1 and 6.2.

$$\hat{x}_{k-1}^{(i)} = \hat{x}_{k-1}^+ \qquad i=0;$$

$$\hat{x}_{k-1}^{(i)} = \hat{x}_{k-1}^+ + (\sqrt{(n+\lambda)P_{k-1}^+})_i \qquad i=1,\ldots,n$$

$$\hat{x}_{k-1}^{(i)} = \hat{x}_{k-1}^+ - (\sqrt{(n+\lambda)P_{k-1}^+})_i \qquad i=n+1,\ldots,2n \tag{6.8}$$

and the corresponding weights are calculated as

$$W_0^{(m)} = \lambda/(n+\lambda)$$
$$W_0^{(c)} = W_0^{(m)} + 1 - \alpha^2 + \beta$$

$$W_i^{(c)} = W_i^{(m)} = 1/2(n+\lambda) \qquad i=1,\ldots,2n \tag{6.9}$$

where α, β and λ are as defined in the Section 6.1.

Time Update

The system gets updated from *k-1* to *k* time step. All the sigma points $\hat{x}_{k-1}^{(i)}$ are propagated through the nonlinear function *f(.)* and *h(.)* and then the corresponding nonlinear sigma points $\hat{x}_k^{(i)}$ are obtained.

$$\hat{x}_k^{(i)} = f(\hat{x}_{k-1}^{(i)}, u_k, t_k)$$

$$\hat{y}_k^{(i)} = h(\hat{x}_k^{(i)}, t_k) \tag{6.10}$$

Using the $\hat{x}_k^{(i)}$ vectors and also the weights $W_i^{(c)}$ and $W_i^{(m)}$ we perform the following steps.

a) the *a priori* state estimate $\hat{x}_k^-$ at time t_k is calculated as in Equation 6.4

$$\hat{x}_k^- = \sum_{i=0}^{2n} W_i^{(m)} \hat{x}_k^{(i)} \tag{6.11}$$

b) the *a priori* estimation error covariance

$$P_k^- = \sum_{i=0}^{2n} W_i^{(c)} (\hat{x}_k^{(i)} - \hat{x}_k^-)(\hat{x}_k^{(i)} - \hat{x}_k^-)^T + Q_{k-1} \tag{6.12}$$

Similarly using the $\hat{y}_k^{(i)}$ vectors (measurements from sigma points) $\hat{y}_k^-$ is calculated as

$$\hat{y}_k^- = \sum_{i=0}^{2n} W_i^{(m)} \hat{y}_k^{(i)} \tag{6.13}$$

Measurement Update

Using the calculated *a priori* state estimate, *a priori* estimation error covariance and measurement estimate, the following terms are calculated.

a) Covariance of the predicted measurement

$$P_{yy} = \sum_{i=0}^{2n} W_i^{(c)} (\hat{y}_k^{(i)} - \hat{y}_k^-)(\hat{y}_k^{(i)} - \hat{y}_k^-)^T + R_k \tag{6.14}$$

b) Now estimate the cross covariance between $\hat{x}_k^-$ and $\hat{y}_k^-$ as

$$P_{xy} = \sum_{i=0}^{2n} W_i^{(c)} (\hat{x}_k^{(i)} - \hat{x}_k^-)(\hat{y}_k^{(i)} - \hat{y}_k^-)^T \tag{6.15}$$

c) The measurement update of the state estimate and estimate error covariance is performed using the general Kalman filter equations by calculating the Kalman gain K_k

$$K_k = P_{xy} P_{yy}^{-1}$$

$$\hat{x}_k^+ = \hat{x}_k^- + K_k (y_k - \hat{y}_k^-)$$

$$P_k^+ = P_k^- - K_k P_{yy} K_k^T \tag{6.16}$$

6.2.2 Algorithm for non-additive noise

The equations derived in the above algorithm are for additive noises (process and measurement noise), but we can implement the same equations with little modification in case the noises are not additive. Consider a discrete time nonlinear system represented by the following equations.

$$\begin{aligned} x_{k+1} &= f(x_k, u_k, w_k, t_k) \\ y_k &= h(x_k, v_k, t_k) \end{aligned} \tag{6.17}$$

w_k and v_k are the process and measurement noises respectively, which are incorporated in to the system and are clearly non additive.

The modifications that are to be made in the above algorithm are:

a) Augment the noise vectors onto the state vector

$$x_k^a = \begin{bmatrix} x_k \\ w_k \\ v_k \end{bmatrix} \tag{6.18}$$

b) The UKF is used to estimate the augmented state x_k^a. For this we need different initial conditions from that of the above derived algorithm.

$$\hat{x}_k^{a+} = \begin{bmatrix} E(x_0) \\ 0 \\ 0 \end{bmatrix}$$

$$P_0^{a+} = \begin{bmatrix} E[(x_0 - \hat{x}_0)(x_0 - \hat{x}_0)^T] & 0 & 0 \\ 0 & Q_0 & 0 \\ 0 & 0 & R_0 \end{bmatrix} \tag{6.19}$$

where x_0, Q_0 and R_0 have the same value as in the previous case.

c) As the UKF estimates the augmented state (both state and noise) instead of only the state vector, the Q_{k-1} term in Equation 6.12 and R_k in Equation 6.14 are removed from the algorithm.

Once these modifications are made, the UKF can be implemented recursively to estimate the state and the covariance.

6.3 Sigma point selection analysis

Sigma points are a set of deterministically chosen points which match the mean and covariance of a probability distribution (not necessarily Gaussian). Sigma points are calculated by the square root decomposition of the estimation error covariance. These are distributed on either side of the state estimate with a value of factor of the square root of the estimation error covariance. In the previously discussed algorithm a total of $2n+1$ sigma points are used. Then, all of the $2n+1$ sigma points are propagated through the nonlinear function (system) to calculate the weighted mean and covariance which in turn approximate the state estimate and error covariance. It is obvious from the above discussion that at each time step, a set of $2n+1$ sigma points are propagated through the nonlinear function. On the other hand, in the EKF the system has to be linearized at each time step to estimate the state and error covariance.

The main computational effort in the UKF is the number of sigma points to be used for the estimation. So it has become very difficult computationally to estimate the states of a higher order system using the UKF. Lots of research is going on in this particular field to reduce the number of sigma points and achieve the same amount of accuracy as with the $2n+1$ sigma points. This research has resulted in the following sets of sigma points.

a) The simplex sigma point set [25]

b) The minimal skew simplex sigma point set [26]

c) The simplex spherical sigma point set [27]

6.3.1 Algorithm for minimal skew simplex sigma point set

It is stated in [25] that given only an n-dimensional mean and covariance estimate, with no other error distribution information, a set of n+1 sigma points can be constructed that fully captures all of the known statistics of the error distribution, i.e., its mean and covariance. This is set is called the s*implex sigma point set.* This is the only set of all possible sets of sigma points which match the statistics of the distribution (mean and covariance) to second order.

However, many filtering and control applications involve the use of a measuring process that introduces errors that can be empirically characterized to some extent. This characterization represents the information regarding the higher moments of distribution like *skew* (third order moment) and *kurtosis* (fourth order moment). But, the simplex sigma point set of *n+1* points does not incorporate the information about these higher order moments. So to overcome this difficulty, a new set of sigma points called the m*inimal skew simplex sigma point set* has been derived to incorporate the information about the third order moment and also to minimize its value. An additional sigma point at the origin transforms the simplex sigma point set to the minimal skew simplex sigma point set. The sigma point selection algorithm for the minima skew simplex sigma point set is as follows.

1) Chose $0 \le W_0 \le 1$

2) Choose the weight sequence:

$$W_i = (1 - W_0)/2^n \qquad i=1$$

$$W_i = W_1 \qquad i=2$$

$$W_i = 2^{i-2} W_1 \qquad i=3,\ldots\ldots,n+1 \tag{6.20}$$

3) Initialize the vector sequence

$$X_0^1 = [0],\ X_1^1 = [-1/\sqrt{2W_1}] \text{ and } X_2^1 = [1/\sqrt{2W_1}] \tag{6.21}$$

4) Expand the vector sequence for $j=2,\ldots\ldots,n$ according to the following equations

$$X_i^{j+1} = \begin{bmatrix} X_0^j \\ 0 \end{bmatrix} \qquad i=0$$

$$X_i^{j+1} = \begin{bmatrix} X_i^j \\ -1/\sqrt{2W_{j+1}} \end{bmatrix} \quad i=1,\ldots\ldots,j$$

$$X_i^{j+1} = \begin{bmatrix} 0_j \\ 1/\sqrt{2W_{j+1}} \end{bmatrix} \quad i=j+1 \tag{6.22}$$

where 0_j represents a zero vector of size jx1.

The estimation accuracy with the minimal simplex sigma point set is the same as with the general symmetric sigma point set of 2n+1 points but with half the computational cost. According to the above algorithm sigma point selection would result in all the sigma points placed on a sphere around the origin (zero-th point) with a radius equal to their corresponding weights [26]. The weights on each point vary by a factor of 2^n and the values on the coordinates of each point vary by a factor of $2^{n/2}$. This weight assignment and value assignment to sigma points would lead to big numerical problems for higher order systems (very high *n).* To overcome this difficulty, a new set of points which have better behavior at higher dimensions was derived.

The new set of points is called the spherical simplex sigma point set [27]. In this set all sigma points lie on origin or on a hypersphere centered at the origin. The following section describes the spherical simplex sigma point set.

6.3.2 Algorithm for spherical simplex sigma point set

1) Choose $0 \le W_0 \le 1$

2) Choose the weight sequence:

$$W_i = (1 - W_0)/(n+1) \tag{6.23}$$

3) Initialize the vector sequence as:

$$X_0^1 = [0],\ X_1^1 = [-1/\sqrt{2W_1}] \text{ and } \quad X_2^1 = [1/\sqrt{2W_1}] \tag{6.24}$$

4) Expand the vector sequence for *j=2,……, n* according to the following equations.

$$X_i^j = \begin{bmatrix} X_0^{j-1} \\ 0 \end{bmatrix} \qquad i=0$$

$$X_i^j = \begin{bmatrix} X_i^{j-1} \\ -1/\sqrt{j(j+1)W_1} \end{bmatrix} \qquad i=1,\ldots\ldots,j$$

$$X_i^j = \begin{bmatrix} 0_{j-1} \\ 1/\sqrt{j(j+1)W_1} \end{bmatrix} \qquad i=j+1 \tag{6.25}$$

where 0_{j-1} represents a zero vector of size *(j-1) ×1*

There are two major differences in this algorithm to that of minimal simplex sigma point set. First, the weight on each sigma point (apart from the 0^{th} point) is the same and proportional to $(1-W_0)/(n+1)$. Second, the sigma points lie on the hypersphere of radius $\sqrt{n}/(1-W_0)$.

6.4 Inverted pendulum application

The UKF derived in the previous sections was applied to estimate the states of the highly nonlinear inverted pendulum which is considered to be a benchmark problem in nonlinear estimation. Consider an inverted pendulum as shown in Figure 6.3.

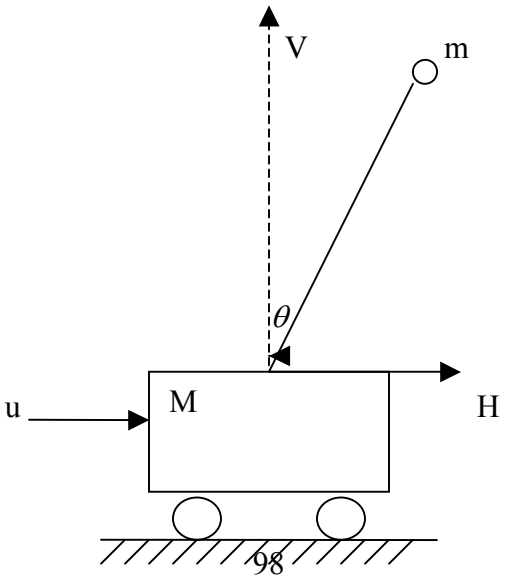

y

Figure 6.3: Inverted Pendulum

This inverted pendulum equipment has cart of mass 1 kg (M) with a pendulum of mass 0.2 kg (m), length 1 meter (l) and radius of 0.02 m (r). This pendulum is mounted in an inverted position. V and H shown in Figure 6.3 are the reaction forces of pivot on pendulum. The angle that pendulum makes with the vertical is represented by θ and the cart position is represented by *y*. The coefficient of viscous friction is taken to be F and u is the input (force) to the cart to move. The following equations represent the behavior of the nonlinear inverted pendulum plant.

1) $u = M\ddot{y} + F\dot{y} + H$

2) $H = m\ddot{y} + ml\ddot{\theta}cos\theta - ml\dot{\theta}^2 sin\theta$

3) $V = mg - ml\ddot{\theta}sin\theta - ml\dot{\theta}^2 cos\theta$

4) $J\ddot{\theta} = Vlsin\theta - Hlcos\theta$

where $J = \frac{mr^2}{2}$, is the moment of inertia of pendulum (*m*), and *g* is the acceleration due to gravity.

Initially the model is linearized by the Taylor series expansion and is represented in state space form as follows. From the system equations, we can consider position of

the cart (*y)*, velocity of the cart ($\dot{y}$), angle of the pendulum with the vertical *(*θ*)* and angular displacement *(*$\dot{\theta}$*)* to be four states of the system that are to be estimated. The control input *(u)* is considered to be a function of angle θ. It is also assumed that the position of the cart can be measured, i.e., *y* is the measurement obtained from the system.

$$\dot{x} = Ax + Bu \tag{6.26a}$$

$$y = Cx + Du \tag{6.26b}$$

where $A = \begin{bmatrix} 0 & 1 & 0 & 0 \\ 0 & -F/M & -mg/M & 0 \\ 0 & 0 & 0 & 1 \\ 0 & F/M/l & (M+m)g/M/l & 0 \end{bmatrix}$, $B = \begin{bmatrix} 0 \\ 1/M \\ 0 \\ -1/Ml \end{bmatrix}$, $C = \begin{bmatrix} 1 & 0 & 0 & 0 \end{bmatrix}$

and *D = 0* since there is no effect of the control on the measurements.

The system is run in open loop with an initial angle of 0.1 radians for 3 sec with a time step of 0.005 sec. The nonlinear simulations are run to plot the true states of the systems. Then the extended Kalman filter and unscented Kalman filter algorithms are implemented to estimate the states of the inverted pendulum. The extended Kalman filter estimates the states using the above calculated Jacobians for the linearization. But the unscented Kalman filter is implemented by running the nonlinear model with the calculated sigma points.

The extended Kalman filter is implemented by calculating the linearized model at every time step. Linearizing the inverted pendulum model at every time step may not

seem to be a big computational effort because they are just four second-order differential equations to be solved, but for a bigger problem like MAPSS it is really cumbersome. On the other hand, the unscented Kalman filter estimates the states by propagating a set of sigma points through the nonlinear system at every time step. There will be 9 sigma points to be propagated at each time step as discussed in Section 6.2 ($2n+1$ sigma points for an nth order system). Similar to the computational effort discussed for the extended Kalman filter, propagating the sigma points through huge systems can be a problem. Implementation of the unscented Kalman filter for MAPSS model is discussed in more detail in Chapter VII.

6.5 Simulation results

Figure 6.4a and 6.4b show the state estimations of the extended Kalman filter and unscented Kalman filter along with the true states over the entire simulation time. Considering the first state from Figure 6.4a, the position of the cart, we can conclude that both estimation techniques were equally good. The reason behind that accuracy is that it was the only state that could be measured. When velocity estimation is considered, it can be seen that the unscented Kalman filter was performing better than the extended Kalman filter after a time of 1.5 seconds. And finally the plots in Figure 6.4b, the last two states estimations, show that the unscented Kalman filter was far better than the extended Kalman filter as time increases. It can be seen that the unscented Kalman filter was tracking the true state over the entire time, but the extended Kalman filter was unable to track the true state after a certain time. The main reason behind the unscented Kalman filter performing better than the extended Kalman filter is that the unscented

transformation approximates the mean to third order which is better than linearization and also approximates the covariance to third order similar to linearization.

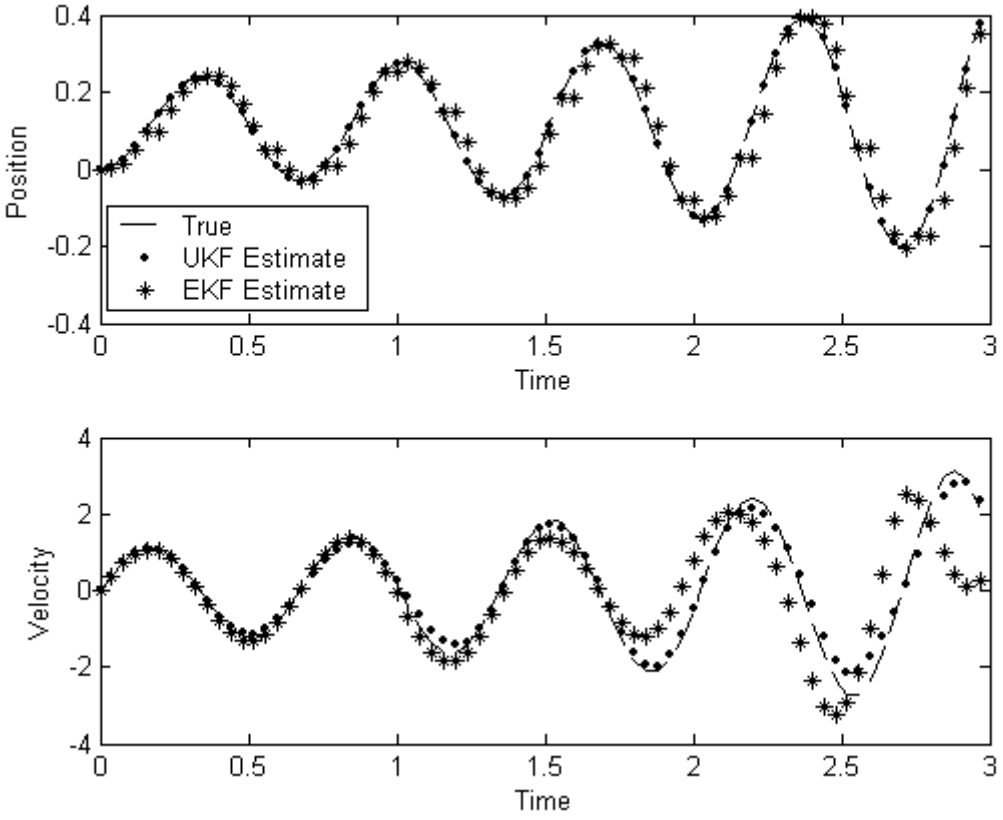

Figure 6.4a: Estimation of position and velocity of the cart

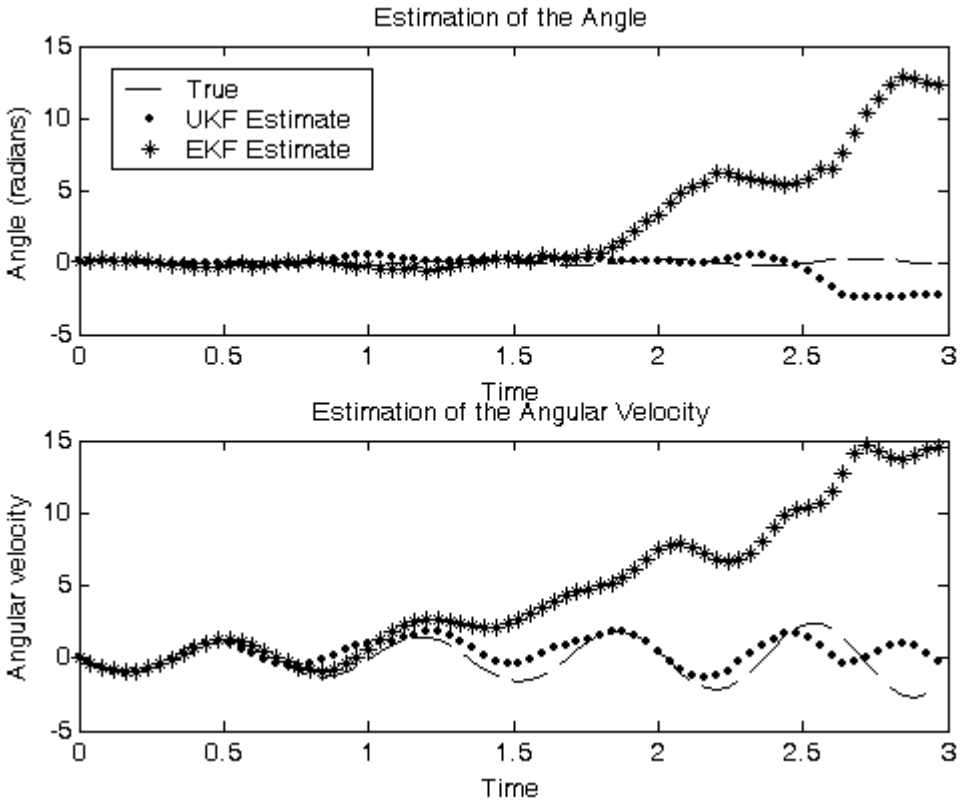

Figure 6.4b: Estimation of angle and angular velocity of the pendulum

CHAPTER VII

CONCLUSIONS AND FUTURE WORK

7.1 Conclusions

The performance of the 27 linearization combinations was investigated. Comparisons were made on the basis of RMS difference between linear and nonlinear models over an entire six-second simulation, RMS difference at the final time of the simulation, and RMS parameter estimation error of a Kalman filter.

When RMS difference (averaged over the entire simulation) between the linear and nonlinear models is considered, the best linearization method is

(1) Steady state error reduction method for state linearization

(2) Matlab method for control linearization.

(3) Steady state error reduction method for health parameter linearization

When RMS difference (at the final time) between the linear and nonlinear models is considered, the best linearization method is

(1) Perturbation method for state linearization

(2) Steady state error reduction method for control linearization.

(3) Steady state error reduction method for health parameter linearization

When Kalman filtering health parameter estimation for the engine operating at ground condition, i.e., first operating condition (with PLA=21, Mach number=0 and altitude=0) is considered, the best linearization method is

(1) Matlab method for state linearization

(2) Steady state error reduction method for control linearization

(3) Perturbation method for health parameter linearization.

When the engine is operated at cruise, i.e., second operating condition (with PLA=35, Mach number=0.8 and altitude=35000) is considered, then best linearization method is

(1) Steady state error reduction method for state linearization

(2) Perturbation method for control linearization

(3) Perturbation method for health parameter linearization.

The linearization combinations mentioned above are considered to be best, but there are other combinations that behaved close to the best. One important conclusion that can be made is that linearizing the nonlinear model in Matlab method gives worst results.

7.2 Future work

Further work could involve more investigations of the effect of linearization on Kalman filtering. This thesis presents the effects only on the first 50 flights. An entire 500-flight investigation may be useful, although the computational effort would be a consideration. We would have to perform 20 Monte Carlo runs of 27 linearization combinations of 500 flights each, once for the unconstrained filter and once for the constrained filter. To be complete we could check three different perturbation amounts for each of the linearization methods. This gives a total of (20 × 27 × 27 × 2) Kalman filter simulations.

Other work for the future could involve reproducing these results for other filtering techniques, such as unscented Kalman filtering or H-infinity filtering. As discussed in Chapter V, the unscented Kalman filter works on the principle of the unscented transformation. It has its own advantages and disadvantages. Linearization of the MAPSS model, the main computational task in linearized Kalman filter estimation technique, can be overcome (reduced) by applying the unscented Kalman filter to MAPSS model. However, the unscented Kalman filter is still more computationally expensive because of the simulations required for state estimate propagation.

Implementing the unscented Kalman filter on MAPSS is not that easy computationally, as it would be required to run the nonlinear model at every time step for 27 times (since $2n+1$ sigma points are propagated through the nonlinear model where n is the number of augmented states to estimated). The nonlinear MAPSS model is simulated

for 6 seconds and the time step considered in estimating the health parameters was 0.1 seconds. This implies that there would be 30 time steps for estimating the health parameters for each flight as the time for one flight is considered to be 3 seconds. So, that would take 30 × 27 MAPSS simulations for estimating the health parameter degradation after one flight. Hence, this is cumbersome to implement computationally. But this should give results that are better than what linearized Kalman filter achieved. The unscented Kalman filter was shown to be working better than the extended Kalman filter for a small state problem (inverted pendulum) in Chapter V.

A MAPSS simulation for 6 seconds would take around 42 seconds of CPU time on a Pentium-IV, 1.8 GHz, 256 MB RAM system. This would take around 472.5 (30 × 27 × 50 × 42 / 3600) hours of CPU time to estimate the health parameter of the turbofan engine for 50 flights. On the other hand, reducing the time step for the estimation of health parameters would result in small numbers to implement the unscented Kalman filter. But, the estimates may not be as good as those obtained with 0.1 second time steps. So, there is a tradeoff to be considered while estimating the states with an unscented Kalman filter for bigger models (large state problems).

Finally, the results obtained with the unscented Kalman filter after the time step reduction should be compared with those obtained with the linearized Kalman filter with similar time step. This would really lead us to decide if the unscented Kalman filter is better than the linearized or extended Kalman filters.

BIBLIOGRAPHY

[1] Santanu Chatterjee and Jonathan Litt, "Online model parameter estimation of jet engine degradation for autonomous propulsion control," NASA TM 2003-212608.

[2] D. Doel, "An assessment of weighted-least-squares-based gas path analysis," ASME Journal of Engineering for Gas Turbines and Power (116) pp. 366-373, April 1994.

[3] H. DePold and F. Gass, "The application of expert systems and neural networks to gas turbine prognostics and diagnostics," ASME Journal of Engineering for Gas Turbines and Power (232) pp. 607-61, Oct. 1999.

[4] A. Volponi, H. DePold, and R. Ganguli, "The use of Kalman filter and neural network methodologies in gas turbine performance diagnostics: a comparative study," Proceedings of ASME TurboExpo 2000, pp. 1-9, May 2000.

[5] T. Kobayashi and Donald L. Simon, "A hybrid neural network-genetic algorithm technique for aircraft engine performance diagnostics," 37th AIAA/ ASME/ SAE/ ASEE Joint Propulsion Conference, July 2001.

[6] Khary I. Parker and Ten-Heui Guo, "Development of a Turbofan Engine Simulation in a Graphical Simulation Environment," NASA TM 2003-212543.

[7] Simon J. Julier and J.K.Uhlmann, "A new extension of the Kalman filter to nonlinear systems," Proceedings of AeroSense: The 11th international symposium on Aerospace/Defense Sensing, Simulation and controls, 1997.

[8] The aircraft gas turbine engine and its operation, United Technologies Corporation, August 1988.

[9] Mark Burleigh, Improvements in aero engine design in the last 50 years, http://students.bath.ac.uk/en2mdb/ass-tj.htm

[10] Dan J. Simon and Donald L. Simon, "Aircraft Turbofan Engine Health Estimation Using Constrained Kalman Filtering," 2003, ASME IGTI Turbo Expo, Atlanta, June 16-19, 2003.

[11] Khary I. Parker and Kevin J. Melcher, "Modular Aero Propulsion System Simulation (MAPSS) User's Guide," NASA TM 2004-212968.

[12] MATLAB, "Getting Started with MATLAB," The Math Works, Inc., 1996

[13] Simulink, "Using Simulink," The Math Works Inc., 2000

[14] Panos J. Antsaklis and Anthony N. Michel, "Linear Systems, " The McGraw-Hill Companies, Inc., 1997

[15] Arthur Gelb, "Applied optimal estimation," The M.I.T press, 1974.

[16] Robert Stengel, "Optimal control and estimation," Dover Publications, New York, 1994.

[17] Kalman R.E., "A New Approach to Linear Filtering and Prediction Problems," Journal of Basic Engineering (ASME), vol. 82D, pp. 35-45, March 1960.

[18] Dan J. Simon, Fundamentals of Kalman Filters, http://academic.csuohio.edu/simond/courses/kalman/

[19] S. Kosanam and D. Simon, "Kalman Filtering with Uncertain Noise Covariances," Intelligent Systems and Control, Honolulu, HI, pp. 375-379, August 2004.

[20] John S. Bay, "Fundamentals of Linear State Space Systems," WCB/ McGraw-Hill Publications, 1999.

[21] B. Anderson and J. Moore, "Optimal Filtering," Prentice Hall, 1979

[22] Simon J. Julier and J.K.Uhlmann, "Unscented Filtering and Nonlinear Estimation," Proceedings of the IEEE, vol.92, no.3, pp. 401-422, March 2004.

[23] E.A. Wan and R.V.Merwe, "The unscented Kalman filter," in Kalman Filtering and Neural Networks (S. Haykin, ed.), John Wiley & Sons, Inc., 2001.

[24] Dan J. Simon, "The unscented Kalman filter," unpublished notes, 2004.

[25] Simon J. Julier and J.K.Uhlmann, "Reduced sigma point filters for the propagation of means and covariances through nonlinear transformations," Proceedings of American Control Conference, vol. 2, pp. 887-892, 2002.

[26] Simon J. Julier, "The scaled unscented transformation," Proceedings of American Control Conference, Anchorage, AK, pp. 4555 - 4559, May 8-10, 2002.

[27] Simon J. Julier, "The spherical simplex unscented transformation," Proceedings of American Control Conference, Denver, Colorado, pp.2430-2434, June 4-6, 2003.

[28] W. Merrill, "Identification of multivariable high-performance turbofan engine dynamics from closed-loop data," AIAA Journal of Guidance, Control and Dynamics (7)6 pp. 677-683, Nov. 1984

[29] Dan J. Simon and Donald L. Simon, "Kalman filtering with inequality constraints for turbofan engine health estimation", submitted for publication.

[30] S. Kosanam, Kalman Filter for Uncertain Noise Covariances, Cleveland State University, Department of Electrical and Computer Engineering, Masters Thesis, 2004.